PŘÍRODOVĚDECKÁ FAKULTA UNIVERZITY KARLOVY
KATEDRA FYZIKÁLNÍ A MAKROMOLEKULÁRNÍ CHEMIE

BAKALÁŘSKÁ PRÁCE

Eva PLUHAŘOVÁ

PRAHA 2008

UNIVERZITA KARLOVA V PRAZE

Přírodovědecká fakulta

Katedra fyzikální a makromolekulární chemie

Bakalářská práce

POČÁTEK SOLVATACE IONTŮ STUDOVANÝ AB INITIO VÝPOČTY: SROVNÁNÍ VODY A METHANOLU

Eva Pluhařová

Školitel: Doc. Mgr. Pavel Jungwirth, Csc.

ÚSTAV ORGANICKÉ CHEMIE A BIOCHEMIE AKADEMIE VĚD ČESKÉ REPUBLIKY

Centrum biomolekul a komplexních molekulových systémů

CHARLES UNIVERSITY IN PRAGUE

Faculty of Science

Department of Physical and Macromolecular Chemistry

Bachelor thesis

THE ONSET OF ION SOLVATION BY AB INITIO CALCULATIONS: COMPARISON BETWEEN WATER AND METHANOL

Eva Pluhařová

Advisor: Doc. Mgr. Pavel Jungwirth, Csc.

INSTITUTE OF ORGANIC CHEMISTRY AND BIOCHEMISTRY

Center for Complex Molecular Systems and Biomolecules

I confirm that I worked out the presented bachelor thesis solely and all the literature used is properly cited.

Prague, 4. 6. 2008 Eva Pluhařová

First I would like to thank professor Jungwirth for guiding me and for his kindness and support. I would also like to thank members of our group for their help, advice and friendship. Working in our team made computational chemistry even more interesting. Next I would like to thank Mrs. Černá for her technical support. The access to the METACentrum supercomputing facilities provided under the research intent MSM6383917201 is highly appreciated. Finally I would like to thank my parents and Jan for their support, tolerance and love.

Contents

1. Introduction

Aqueous solvation of ions plays an important role in a wide range of chemical and biological systems. From the macroscopic point of view ion solvation seems to be well understood, without any controversy. But if we look at this field at the molecular level either using theoretical methods (molecular dynamics and ab initio calculations) or experimental techniques, we still find some unresolved issues. Over the past three decades the study of both positive and negative gas phase cluster ions has made significant contributions to such scientific diverse fields as atmospheric chemistry, gas phase ion chemistry, surface science, and catalysis. Clusters consisting of simple ions (Cl^-, F^-, and Na^+) and common polar solvents (water and methanol) will be presented in this work. All of these systems show interesting trends in thermochemical data if the ion, the solvent molecule, or number of solvent molecules is changed.

In this work ion solvation processes in water and methanol size selected cluster are systematically compared to each other. The goal of present study is to address this issue by means of accurate ab initio calculations.

The rest of section 1 gives more examples of the importance of ion solvation and presents clusters as a bridge between the gas and the condensed phases. In section 2 we describe employed computational methods, section 3 outlines properties of investigated clusters and section 4 characterizes calculations in details. Section 5 reports the results and compares them with previous studies and section 6 provides conclusion.

1.1. Nature and importance of ion solvation

Ion solvation occurs intrinsically at the microscopic level. The nature of solvation depends on the interplay between ion-solvent and solvent – solvent interactions. The magnitude and directionality, as well as the competition between these two interactions ultimately determine the solvent structure around the ion, thereby leading to solubility (or insolubility) of salts in different solvents, the specificity of various ionophores, and the ion-selectivity of ion channels[1].

1.2. From clusters to bulk

Cluster ions represent an aggregated state of matter, having properties midway between the gas and the condensed phases. Small clusters can serve as models for larger bulk systems for both experimental and theoretical studies. Investigations of the formation and

properties of clusters of increasing size offer a deep insight into the molecular interactions and a possibility to study the molecular details of the change from the gaseous phase to the condensed phase[2]. Experimental and theoretical studies allow extrapolation of some properties from finite systems (clusters) to the infinite bulk.

The simplest model for the description of ion solvation in the bulk is due to Born model. Gibbs energies of solvation of individual ions may be estimated from an equation, where ΔG^0_{solv} is defined with the electrostatic work connected with transferring an ion from vacuum into the solvent, which is treated as a continuous dielectric of relative permittivity ε_r:

$$\Delta G^0_{solv} = -\frac{z_i{}^2 e^2}{8\pi\varepsilon_0 \cdot r_i}\left(1-\frac{1}{\varepsilon_r}\right), \qquad (1)$$

where z_i is the charge number and r_i is the radius of ion.

One can deduce from eq. (1) that interaction of ion with a solvent of higher relative permittivity is stronger than for that with lower relative permittivity. But is it true also for clusters of all sizes? More precisely, we ask ourselves following question: If one has two solvents of very different dielectric constant, such as water with ε_r = 80 and methanol with ε_r = 33, would better ion solvation in the bulk medium with higher dielectric constant translate to stronger interactions in the corresponding small clusters?

2. Theoretical Methods

The Hartree-Fock method, Møller – Plesset perturbation theory and Coupled cluster methods are briefly characterized in this section. Definitions and notation were taken form Cramer's textbook[40].

2.1. Hartree – Fock approximation

Hartree-Fock (HF) theory is fundamental to much of electronic structure theory. It often provides a good starting point for more elaborate theoretical methods which are better approximations to the electronic Schrödinger equation. HF method assumes that the exact, N-body wave function of the system can be approximated by a single Slater determinant Ψ of N spin-orbitals, which is the simplest antisymmetric wave function.

$$\Psi = \frac{1}{\sqrt{N!}} \cdot \begin{vmatrix} \chi_1(1) & \chi_2(1) & \cdots & \chi_N(1) \\ \chi_1(2) & \chi_2(2) & \cdots & \chi_N(2) \\ \vdots & \vdots & \ddots & \vdots \\ \chi_1(N) & \chi_2(N) & \cdots & \chi_N(N) \end{vmatrix}. \tag{2}$$

A more compact notation that finds a widespread use

$$\Psi = \left| \chi_1 \chi_2 \chi_3 \cdots \chi_N \right\rangle. \tag{3}$$

We are looking for the best wave function in this form to describe the ground state of the system. The lowest possible energy is E_0. Variational principle tells us that if we pick any trial wave function Φ to be operated on by the Hamiltonian $\hat{H}$, we will get the following inequality

$$\frac{\left\langle \Phi \middle| \hat{H} \middle| \Phi \right\rangle}{\left\langle \Phi \mid \Phi \right\rangle} \geq E_0. \tag{4}$$

This implies that the best normalized single-determinant wave function is that with the lowest value of the integral in equation (4), the best wave function is obtained by minimization of this integral.

The HF model encompasses the Born – Oppenheimer approximation. It also implies the mean field approximation, which means replacing all interactions between electrons by interaction of each electron with an averaged field of all of the other electrons.

The one electron Fock operator is defined for each electron *i* as

$$\hat{f}_i = -\frac{\hbar^2}{2 \cdot m_e}\Delta_i - \frac{e^2}{4\pi\varepsilon_0}\sum_k^{nuclei}\frac{Z_k}{r_{ik}} + \hat{V}_i^{HF}\{j\}, \tag{5}$$

where Δ_i is Laplace operator, Z_k is the charge of the nucleus, r_{ik} is the distance between electron and nucleus. An effective one-electron potential operator called the Hartree-Fock potential $\hat{V}_i^{HF}\{j\}$ reads:

$$\hat{V}_i^{HF}\{j\} = \sum_{j\neq i}^{N}\hat{J}_j - \hat{K}_j\,. \tag{6}$$

Pseudo one-electron operators $\hat{J}_j$ and $\hat{K}_j$ are called the Coulomb and the exchange operator. These operators are defined by their effect when operating on a spin orbital χ_i. HF canonical orbitals are solution of the eigenvalue equation:

$$\hat{f}_i\chi_i = \varepsilon_i \cdot \chi_i\,, \tag{7}$$

where χ_i is one-electron wave function.

The HF model neglects and "instantaneous" electron repulsion. The difference between converged HF energy and the exact non-relativistic energy E is called electron correlation energy:

$$E^{corr} = E - E^{HF}\,. \tag{8}$$

2.2. Møller – Plesset perturbation theory

Møller-Plesset perturbation theory (MP) is one of several post-Hartree-Fock methods. It improves the Hartree-Fock method by adding electron correlation effects by means of perturbation theory. HF problem can be solved to arbitrary precision, upon extending the basis set. We therefore have a "zero-order" problem together with a perturbation.

$$\hat{H} = \hat{H}^{(0)} + \lambda \cdot \hat{V}\,, \tag{9}$$

where $\hat{H}$ is the full Hamiltonian, $\hat{H}^{(0)}$ is the Hartree-Fock Hamiltonian, λ is a dimensionless parameter, and $\hat{V}$ is a perturbing operator.

$$\hat{V} = \sum_i^{occ}\sum_{j>i}^{occ}\frac{1}{r_{ij}} - \sum_i^{occ}\sum_{j>i}^{occ}\left(J_{ij} - \frac{1}{2}\cdot K_{ij}\right). \tag{10}$$

The first electron-electron electron repulsion, while the second term is the sum over the Fock operators.

Hartree-Fock energy is correct up to the first-order Møller-Plesset perturbation theory. The second order formula is written on basis of doubly excited Slater determinants. They are generated by promoting electrons from occupied orbitals *i, j* to virtual orbitals *a, b*.

Integrals involving doubly excited determinants read as:

$$\sum_{j>0}\left\langle \Psi_j^{(0)}\middle|\hat{V}\middle|\Psi_0^{(0)}\right\rangle = \sum_{i}^{occ}\sum_{j>i}^{occ}\sum_{a}^{vir}\sum_{b>a}^{vir}\left[(ij\mid ab)-(ia\mid jb)\right]^2 . \tag{11}$$

The full expression for the second-order energy correction $a^{(2)}$ is

$$a^{(2)} = \sum_{i}^{occ}\sum_{j>i}^{occ}\sum_{a}^{vir}\sum_{b>a}^{vir}\frac{\left[(ij\mid ab)-(ia\mid jb)\right]^2}{\varepsilon_i+\varepsilon_j-\varepsilon_a-\varepsilon_b}, \tag{12}$$

where ε are the corresponding orbital energies. Sum of the Hartree-Fock energy and $a^{(2)}$ defines the MP2 energy.

MP2 calculations can be done reasonably fast, analytic gradients and derivatives are available for this level of theory. Note, however, that the MPn methodology is only conditionally convergent and is not variational.

2.3. Coupled cluster methods

Coupled cluster is a technique for accurately estimating the electron correlation energy. The fundamental equation relates a HF wave function Ψ_{HF} to the best possible wave function by

$$\Psi = e^{\hat{T}}\Psi_{\mathrm{HF}}. \tag{13}$$

The exponential operator is defined by a Taylor-series expansion:

$$e^{\hat{T}} = \sum_{k=0}^{\infty}\frac{\hat{T}^k}{k!}. \tag{14}$$

The cluster operator $\hat{T}$ is defined as

$$\hat{T} = \hat{T}_1 + \hat{T}_2 + \hat{T}_3 + \cdots \hat{T}_n, \tag{15}$$

where n is the total number of electrons and the various $\hat{T}_i$ operators generate all possible determinants having i excitations from the reference.

The coupled cluster energy E_{CC} is computed as

$$E_{CC} = \left\langle \Psi_{\mathrm{HF}}\middle|e^{-\hat{T}}\hat{H}e^{\hat{T}}\middle|\Psi_{\mathrm{HF}}\right\rangle. \tag{16}$$

It is usual to approximate the $\hat{T}$ operator by including only some of the terms and it is generally accepted that the most important contribution is $\hat{T}_2$. We make the approximation $\hat{T} = \hat{T}_2$ which gives the coupled cluster doubles (CCD) method:

$$\Psi_{CCD} = \left(1 + \hat{T}_2 + \frac{\hat{T}_2^{\,2}}{2!} + \cdots\right)\Psi_{\mathrm{HF}}. \tag{17}$$

The next step is to include the $\hat{T}_1$ operator and so take $\hat{T} = \hat{T}_1 + \hat{T}_2$ which provides the CCSD method. The scaling behavior of CCSD is of the order of N^6, where N is the number of electrons. Inclusion of connected triple excitations $\hat{T} = \hat{T}_1 + \hat{T}_2 + \hat{T}_3$ defines CCSDT, but it is very computational costly (scaling as N^8). Various approaches to estimating the effect of connected triples using perturbation theory have been proposed, the most robust being the CCSD(T) method, which also includes a singles/triples coupling term. The triples contribution is calculated via perturbation theory (formula given by MP4). CCSD(T) method is sometimes called the gold standard of quantum chemistry.

2.4. Basis set

The basis set is the set of mathematical functions from which the wave function is constructed. Each molecular orbital (MO) in HF theory is expressed as linear combination of basis functions, the coefficients for which are determined iteratively. It is useful to choose basis set functional forms that permit the various integral to be evaluated in a computationally efficient fashion. Basis functions must be also chosen such as to have a form that is useful in a chemical sense.

Slater-type orbitals (STOs) closely resemble hydrogenic atomic orbitals, the radial decay of the STOs being proportional to e^{-r}. But there is no analytical solution available for the general four-index integral when the basis functions are STOs. If the radial decay is changed from e^{-r} to e^{-r^2}, we obtain Gaussian-type orbitals (GTOs) for which analytical solution of four-index integral exists, but they do not have the proper radial shape. In order to combine the best features of both, most of the first basis sets development used GTOs as building blocks to approximated STOs, however, this basis set approach abandoned later. When a basis function is defined as a linear combination of Gaussians, it is called a contracted basis function. Pople and co-workers systematically determined the contraction coefficients and GTOs[43-45].

For more accurate results, one needs more flexible basis sets, which should be decontracted. A basis set with X functions for each atomic orbital (AO) is called a X-ζ basis. Core orbitals are usually not decontracted, because they are weakly affected by chemical bonding. Dunning and co-workers developed cc-pVXZ sets, where the acronym means correlation-consistent polarized Valence X (Double, Triple…) ζ. Correlation consistent means that contraction coefficients were variationally optimized not only for HF, but also for calculations including electron correlation.

The highest energy MOs of anions, highly excited electronic states, and loose supermolecular complexes tend to be more spatially diffuse. Diffuse "augmented" basis function should be added to describe these orbitals correctly. For example diffuse functions in Dunnig's basis[42] set are indicated by prefix aug.

2.5. Interaction energy

If we consider a complex A – B, we can quantify the strength of the interaction between subsystems A and B by calculating the energy difference of the complex and subsystems:

$$\Delta E = E(A-B) - E(A) - E(B). \tag{18}$$

This definition is not unambiguous. We should specify geometry of subsystems A and B, because geometry of each partner is slightly different when it is isolated and in the complex.

2.5.1. Basis set superposition error

A useful definition of interaction energy for complex A – B reads:

$$\Delta E = E^{a\cup b}(A-B)_{A-B} - E^{a}(A)_{A-B} - E^{b}(B)_{A-B}, \tag{19}$$

where *a, b* are the basis functions associated with components A, B and A-B means the geometry of the complex. *a, b* are not complete basis sets, so there are more basis functions employed in the calculation of the complex, which can provide an artificial lowering of the energy of the complex, because one of the monomers "borrows" basis functions of the other to improve its own wave function. This can be corrected by counterpoise (CP) scheme:

$$\Delta E = E^{a\cup b}(A-B)_{A-B} - E^{a\cup b}(A)_{A-B} - E^{a\cup b}(B)_{A-B}. \tag{20}$$

This is the energy of bringing monomers together, each having the same geometry as in the complex. In the monomeric calculations, basis function of the missing partner are included in the calculation.

2.5.2. Vertical dissociation energy

When calculating vertical dissociation energy we assume that the process of dissociation is so fast that geometry of each subsystem does not change. This energy is calculated using equation (20), but it has opposite sign, (association vs. dissociation).

2.5.3. Adiabatic dissociation energy

While calculating vertical dissociation energy we assume that relaxation of subsystems during dissociation is so fast that geometry of each subsystem is its optimized structure. Note however, that according to the uncertainty principle nuclei are not located exactly at certain positions, and the motion of nuclei is "tied up" in molecular vibrations.

Zero-point vibrational energy is defined as a sum of the energies of the lowest vibrational levels over all molecular vibrations. The internal energy of a molecule at 0 K is:

$$U_0 = E_{el} + ZPVE\,. \tag{21}$$

We evaluate the adiabatic dissociation energy using equation:

$$\Delta E = E_{el}(A) + ZPVE(A) + E_{el}(B) + ZPVE(B) - E_{el}(A-B) - ZPVE(A-B). \tag{22}$$

2.5.4. Extrapolation scheme

Basis-set convergence and extrapolations are among important issues of contemporary molecular ab initio theory. For total energies, it is well known that the convergence of the correlation part is significantly slower than for the Hartree-Fock part. This suggests that one should treat the HF and correlation parts separately.

For convergence of the correlation energy $E_{\mathrm{X}}^{\mathrm{corr}}$ Helgaker et al[4] used the expression

$$E_{\mathrm{X}}^{\mathrm{corr}} = E_{\mathrm{CBS}}^{\mathrm{corr}} + A \cdot X^{-3}\,. \tag{23}$$

For convergence of HF energy they mentioned two extrapolation forms;
an exponential:

$$E_{\mathrm{X}}^{\mathrm{HF}} = E_{\mathrm{CBS}}^{\mathrm{HF}} + B \cdot \exp(-\alpha \cdot X) \tag{24}$$

and power:

$$E_{\mathrm{X}}^{\mathrm{HF}} = E_{\mathrm{CBS}}^{\mathrm{HF}} + B \cdot X^{-\alpha}\,. \tag{25}$$

Here, we considered the HF energy to be converged, so nor eq. (24) neither eq. (25) were used. Complete basis set (CBS) MP2 energies were estimated using a two-point scheme derived from eq. (23):

$$E_{\mathrm{CBS}}^{\mathrm{MP2}} = E_{\mathrm{X_1}}^{\mathrm{MP2}} + \frac{E_{\mathrm{X_2}}^{\mathrm{MP2}} - E_{\mathrm{X_1}}^{\mathrm{MP2}}}{\frac{\left(X_2/X_1\right)^3 - 1}{\left(X_2/X_1\right)^3}}, \tag{26}$$

where X_1 and X_2 are cardinal numbers of Dunning's basis set (aug-cc-pVXZ) and $E_{\mathrm{X_1}}^{\mathrm{MP2}}$ and $E_{\mathrm{X_2}}^{\mathrm{MP2}}$ are MP2 energies calculated employing these basis sets. Assuming that the difference between CCSD(T) and MP2 energies exhibits only a small basis set dependence[5,6] CBS CCSD(T) energies can be estimated as:

$$E_{\mathrm{CBS}}^{\mathrm{CCSD(T)}} = E_{\mathrm{CBS}}^{\mathrm{MP2}} + \left(E_X^{\mathrm{CCSD(T)}} - E_X^{\mathrm{MP2}}\right). \tag{27}$$

3. Microscopic Solvation of Ions by Water and Methanol

Microscopic solvation of ions by polar solvent molecules has been studied during last few decades both experimentally [1,7,12-25] and theoretically [1,8-10,27-39]. Here, we briefly review this issue. Results of previous studies will be compared with present calculations in section 5.6.

3.1. Surface vs. interior solvation

In ion-solvent clusters, solvation structures fall into two basic categories: interior and surface ion geometries. Interior solvation occurs when the ion is at or near the center of the mass of the cluster, leading to a quasi-symmetric structure. For surface solvation, the structure is asymmetric, with the solvent molecules aggregating on one side of the ion. Discussion about surface and interior solvation is especially relevant for halide hydration. Classical simulation studies[32,33,37] have suggested that the halide ions (except for F^-) reside at the surface of neutral water cluster. The main questions concern the role of ion and solvent properties in this phenomenon, particularly polarizability and hydrogen bonding.

3.2. Experimental studies

Vibrational spectroscopy is a sensitive, size specific probe of hydrogen bonding in both ionic and neutral clusters. Fluoride, chloride, and sodium in small to medium sized clusters were studied by vibrational predissociation spectroscopy[1,7,12-14]. The ions of interest are generated and then guided into a molecular beam expansion of the desired solvent molecule in source chamber. The ions collide with the neutral solvent clusters and become solvated on a picoseconds timescale, acquiring a significant amount of internal energy due to the initial collision and the exothermic solvation process. These “hot” clusters stabilize by evaporative cooling and product clusters $Ion(Sol)_n$ are then analyzed by a quadrupole mass spectrometer.

A tunable infrared laser is used for vibrational excitation of the cluster ion of interest (selected by the first quadrupole) leading to a loss of a solvent molecule (via vibrational predissociation). This results in an increase in the number of the $Ion(Solvent)_{n-1}$ fragment ions which are contained by the second ion-guiding quadrupole and subsequently detected by the third quadrupole.

The infrared spectrum of a cluster Ion(Solvent)$_n$ is collected by monitoring the increase in dissociation into a specific loss channel at various laser frequencies. Frequency shifts of the solvent O-H stretch are used to identify both the hydrogen bond formation and the nature of the hydrogen bonded species in the cluster ion. These studies are focused on hydrogen bonding network, which can give us reliable information about the type of solvation (surface vs. interior). Stepwise dissociation (or association) enthalpies are determined by different experimental techniques.

On of them is the high pressure mass spectrometry (HPMS) which has been used for studying clustering reactions of both cations and anions[15-20]. First ions are formed; e. g. halide ions are prepared in a high pressure region (1-20 Torr) by dissociative electron attachment. Widely used electron capture agents are NF_3 and CCl_4. Sodium ions are formed by thermionic emission from a resistively heated platinum filament coated with sodium nitrate. The reaction mixture consists of less than 15% solvent in a buffer gas; it is important to know the exact value of partial pressure of the clustering agent and also to ensure that equilibrium is established. The equilibrium constant is calculated from the ratio of the measured ion intensities and known partial pressure of the clustering solvent. A number of such measurements at various temperatures results in a van't Hoff plot from which enthalpy and entropy changes for a particular clustering reaction can be determined. Bogdanov[21] et al used modification of this method called pulsed-ionization high pressure mass spectrometry (PHPMS).

Dunbar[22] and coworkers studied the kinetics of dissociation of $Cl^-(H_2O)_2$ and $Cl^-(H_2O)_3$ at essentially zero-pressure by absorption of infrared photons from the background radiation field (ZTRID). The kinetics of this process is highly sensitive to the dissociation enthalpies of the ionic complexes. Enthalpies of interest can be determined from temperature dependence of dissociation rate.

Another technique is collision-induced dissociation (CID) which has been used for determining of absolute binding energies of sodium ions to water, short chain alcohols and other small organic molecules containing electronegative atoms [23-25]. The complexes are formed by associative reactions of sodium cation with neutral solvent. Collisions with buffer gas thermalize the ions both vibrationally and rotationally. The most favorable process observed for all complexes is the loss of an intact ligand in CID which is induced by Xenon atoms. Binding energies can be obtained by thermochemical analysis of each of these steps.

3.3. Theoretical studies

Theoretical studies often accompany experimental investigations based on vibrational spectroscopy[1,14,26]. The goal of theoretical parts of these studies is to find optimized structures of clusters of interest and compare them with results from interpretation of measured spectra. An important task is to establish the type of solvation (symmetric or asymmetric).

Structures of halide(F^-,Cl^-)-water clusters have been studied using post HF methods by Xantheas[9,10,28,29], Masamura[8], Combariza[27,32,33] and other authors[11,30,31]. Not only global minima, but also other low lying structures and transition states are presented in these articles. Xantheas investigated harmonic vibrational frequencies and incremental association enthalpies. The last above mentioned article focused on determination of fluoride-water bond energy, since there still exists discrepancy between theory and experiment. Masamura showed that relative stability of the $Cl^-(H_2O)_n$ isomers is significantly different from that of the corresponding $F^-(H_2O)_n$ isomers; he also calculated infrared spectra of several isomers. Hall et all[34] tested the ability of density functionals to describe aqueous solvation, performing MP2 and CCSD(T) calculations as a benchmark. They did not identify a universal functional suitable for calculation of hydration of different kinds of species. Nevertheless, for example B3LYP gives reasonable results for halide hydration. Structures and energetics of halide-alcohol clusters were studied at MP2 and B3LYP level of theory by Bognanov[38]. Lithium and sodium-methanol clusters were described at the same levels of theory[39].

Classical Monte Carlo simulations[35], Monte Carlo simulations employing effective fragment potentials[36] and molecular dynamics simulations[31,37] were also used for characterizing halide-water complexes and calculating total binding energies and incremental association enthalpies. These techniques in general can provide connection between ab initio results at 0 K and behavior of the system at room temperature. The dominant isomer at room temperature is not necessarily the energetically most stable one, since entropy can play very important role. Identification of number of water molecules which are required to fully surround each anion and comparison of stability of surface and interior isomers was done.

3.4. Summary of previous studies

Small water clusters with halide anion or alkali cation have been studied extensively in the last decades. Alkali cations such as sodium or potassium typically exhibit a roughly symmetric water solvent shell. Studies of microhydration of halides show a gradual build-up of an asymmetric solvent shell around the anion. Only fluoride exhibits a more symmetric

mode of hydration. Ion-methanol clusters have been also studied in order to provide a deeper insight into the solvation of ions in polar solvents. Methanol molecules surround the central cation symmetrically to form interior ion structure. No solvent-solvent hydrogen bonds can be formed in clusters containing up to four methanol molecules, this fact is true also for small water clusters.

Solvation of fluoride anion is not as simple as solvation of cations. For example, the minimum energy structure of $F^-(H_2O)_2$ is bent, but linear transition state structures are energetically very close. The minimum energy structure of $F^-(H_2O)_3$ is pyramidal, but after ZPVE correction the symmetric transition state lies below it. It can be concluded that internal structures compete with surface ones and at room temperature entropic effects favor internal structures[11]. Fluoride anion was observed to be internally hydrated with three to five water molecules. These results contrast with the fact that fluoride anion is surface solvated in methanol and the first evidence for methanol-methanol hydrogen bond appears when fluoride is solvated by four methanol molecules. Both experimental and theoretical studies concerned with chloride hydration show presence of strong ionic hydrogen bonds together with a clear evidence of water – water hydrogen bonding networks in clusters containing four and more water molecules. Data suggest that chloride is surface solvated in water as well as methanol clusters. The type of solvation of above mentioned ions by water and methanol is similar, indicating that the nature of the ion may be primarily responsible for the symmetric or asymmetric solvation. The nature of the solvent does not appear to play such an important role in the type of solvation, with the possible exception of fluoride.

For describing the potential between an ion and a neutral molecule at a relatively large distance, we can use the classical equation[41] (28), which can be called ion-induced dipole and ion-dipole model:

$$V(r) = -\frac{\alpha \cdot q^2}{2 \cdot r^4} - \frac{q \cdot \mu_D}{r^2} \cdot \cos\theta(r). \qquad (28)$$

It can serve as a first approximation for obtaining relative solvation energies. In eq. (28), α is the molecular polarizability, q is the electronic charge on the ion, μ_D is the dipole moment of the solvent molecule, θ is the angle between the line of centers of the ion and the neutral and dipole moment of the solvent, and r is the distance of separation between the ion and neutral. The importance of dipole moment and polarizability of solvent molecule will be discussed for specific examples.

Sodium is bound more strongly to methanol than to water. Replacement of a water molecule with methanol is exothermic for small cation-solent clusters, but this exothermicity

decreases with the increasing total number of ligands. This is ascribed to the increase in distance between the metal ion and the ligands, which underlines the importance of the larger permanent dipole moment of water, relative to the larger polarizability of methanol[20]. For binding of halides to water and alcohols, we can find the same trend as for sodium. It can be concluded that the ion-induced dipole term is mainly responsible for the increase of dissociation energy of complexes of halides with alcohols with increasing length of carbon chain[21].

Experimental and theoretical results are consistent in general trends, meaning that ions bind stronger to methanol than to water in small clusters. But values of binding energies obtained from theoretical calculations and various experimental techniques slightly differ.

4. Calculations

4.1. Investigated systems

Ab initio calculations were performed for small aqueous and methanolic clusters containing sodium cation and fluoride and chloride anion. Clusters consisted of one ion and one, two, or three molecules of solvents. To obtain adiabatic dissociation energies of ions (see paragraph 4.3) it was necessary to carry out calculations for isolated solvent molecules and clusters containing two or three molecules of the solvent. This was also useful for comparison between the structure of an isolated solvent molecule and its geometry in several kinds of clusters.

4.2. Geometry optimization

Structures of all clusters were determined by gradient optimization using MP2 method with aug-cc-pVDZ and aug-cc-pVTZ basis sets. HF method with 3-21g basis set was used for pre-optimization. Stationary points were verified to be to be minima via standard frequency calculations (positive Hessian eigenvalues for all vibrational modes indicated minimum) which were also used to calculate zero-point vibrational energy.

4.3. Interaction energy

Knowledge of dissociation energies is important for comparison of computational and experimental results. To characterize the clusters, the following dissociation energies were calculated: vertical and adiabatic dissociation energies of a solvent molecule, and vertical and adiabatic dissociation energies of the ion. The first two energies are connected with this process:

$$\mathrm{Ion(Solvent)_n} \rightarrow \mathrm{Ion(Solvent)_{n-1}} + \mathrm{Solvent}. \qquad (29)$$

Structures of $\mathrm{Ion(Solvent)_{n-1}}$ and Solvent, which were not re-optimized, but had the same geometry as in the optimized cluster $\mathrm{Ion(Solvent)_n}$, were used for calculating vertical dissociation energy. Calculated values are BSSE corrected; this approach was described in paragraphs 2.5.1 and 2.5.2.

For calculation of adiabatic dissociation energy optimized structures of $\mathrm{Ion(Solvent)_{n-1}}$ and Solvent were used and calculated values were ZPVE corrected, (this approach was

described in paragraph 2.5.3). Results show, how strongly a solvent molecule binds to the cluster.

Vertical and adiabatic dissociation energies of an ion are connected with the following process:

$$\mathrm{Ion(Solvent)_n} \rightarrow \mathrm{(Solvent)_n} + \mathrm{Ion}. \tag{30}$$

Structure of $\mathrm{(Solvent)_n}$, which was not optimized, but had the same geometry as in the optimized cluster $\mathrm{Ion(Solvent)_n}$, was used for calculating vertical dissociation energy. Calculated values were BSSE corrected. For calculating adiabatic dissociation energy the optimized structure of $\mathrm{(Solvent)_n}$ was used and calculated values were ZPVE corrected. Results show, how strongly an ion binds to the cluster.

4.4. Extrapolations

Vertical and adiabatic dissociation energies of all clusters were calculated at the MP2/aug-cc-pVXZ, X = 2, 3 and CCSD(T)/ aug-cc-pVDZ level of theory. Extrapolations of electronic energies of species of interest were carried out. In case of adiabatic dissociation energy, the difference of total electronic energies was corrected by ZPVE calculated at MP2/aug-cc-pVTZ, since geometry was also optimized at this level of theory.

To convince ourselves that the extrapolation scheme is working properly, vertical dissociation energies of clusters containing only one solvent molecule were calculated using MP2/ aug-cc-pVXZ, X = 2 – 5 and CCSD(T)/aug-cc-pVXZ, X = 2 , 3 and 4 for complexes containing water. Several extrapolations were carried out. First, we mention a scheme which was then employed for all clusters:

$$E_{\mathrm{CBS}}^{\mathrm{MP2}} = E_{\text{aug-cc-pVDZ}}^{\mathrm{MP2}} + (E_{\text{aug-cc-pVTZ}}^{\mathrm{MP2}} - E_{\text{aug-cc-pVDZ}}^{\mathrm{MP2}}) / 0.703704 \tag{31}$$

and

$$E_{\mathrm{CBS}}^{\mathrm{CCSD(T)}} = E_{\mathrm{CBS}}^{\mathrm{MP2}} + \left(E_{\text{aug-cc-pVDZ}}^{\mathrm{CCSD(T)}} - E_{\text{aug-cc-pVDZ}}^{\mathrm{MP2}}\right). \tag{32}$$

Values of extrapolated energy can also be obtained form Helgaker's two point extrapolation scheme using energies calculated in larger basis set:

$$E_{\mathrm{CBS}}^{\mathrm{MP2}} = E_{\text{aug-cc-pVTZ}}^{\mathrm{MP2}} + (E_{\text{aug-cc-pVQZ}}^{\mathrm{MP2}} - E_{\text{aug-cc-pVTZ}}^{\mathrm{MP2}}) / 0.578125 \tag{33}$$

and

$$E_{\mathrm{CBS}}^{\mathrm{MP2}} = E_{\text{aug-cc-pVQZ}}^{\mathrm{MP2}} + (E_{\text{aug-cc-pV5Z}}^{\mathrm{MP2}} - E_{\text{aug-cc-pVQZ}}^{\mathrm{MP2}}) / 0.488\,. \tag{34}$$

The extrapolation scheme (23) was also tested.

Equations (31, 33, 34) are the results of substitution in eq. (23) assuming that HF energy is converged and correlation energy is given by the difference of MP2 and HF energies. The same procedure can be performed also for CCSD(T) energies. Extrapolations according to equation (31) and (32) as well as fitting all three values in case of the smallest water clusters were carried out. Because of computational cost, ZPVE correction for clusters containing three molecules of methanol were not calculated utilizing augmented basis functions on all atoms, but only on the anion for negatively charged clusters or on oxygen atoms for cluster containing sodium cation. It is common to present energy difference connected with above mentioned processes in terms of association energy (negative values) rather than in terms of dissociation energy. Therefore results in the next section are presented in terms of association energies.

All calculations were performed using Gaussian 03 program[3].

5. Results and Discussion

This section is divided into several parts. The first two consist of figures of optimized solvent cluster structures obtained at the MP2/aug-cc-pVTZ level of theory, tables containing important angles and bond lengths and graphs showing convergence of total electronic energy. Next three sections contain figures of optimized cluster structures and several graphs which illustrate the convergence of total electronic energy and basis dependence of vertical and adiabatic association energy for clusters containing one solvent molecule. The goal of this work are calculations of interaction energy, which are summarized here. The last section compares calculated values and experimental data (whenever available).

5.1. Water clusters

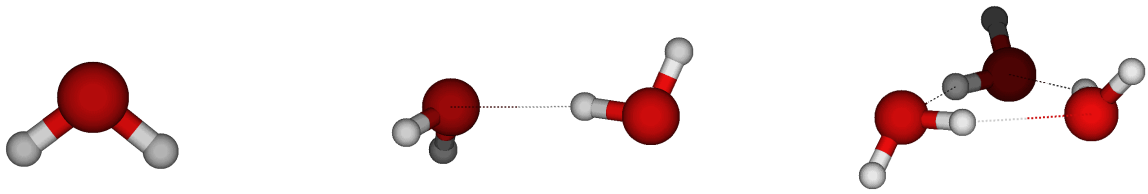

H_2O $(H_2O)_2$ $(H_2O)_3$

Figure 1 Water clusters

Table 1 Bond lengths and angles in $(H_2O)_n$

n	1	2		3		
|OH| water (Å)	0.961	0.969	-	0.975	0.974	0.975
angle HOH water (deg)	104.1	104.5	104.5	105.3	105.6	105.5
|OH| H-bond (Å)	-	1.947	-	1.891	1.911	1.892
angle OHO H-bond (deg)	-	172.2	-	151.1	148.5	151.2

Figure 1 shows small water clusters. Water forms dimer containing one hydrogen bond and cyclic trimer with three hydrogen bonds. Table 1 summarizes geometrical properties of investigated water clusters. The length of covalent OH bond of water (in the second row) is the distance between oxygen and hydrogen which acts as a donor in hydrogen bond. The length of covalent OH bond in water dimer is longer than that of isolated water molecule, but shorter than in water trimer. Hydrogen bond in water dimer (1.95 Å) is longer than in water trimer (1.90 Å). Values in this table can be compared with values obtained for clusters

containing ions and give us qualitative information about the strength of solvent-solvent and ion-solvent interactions.

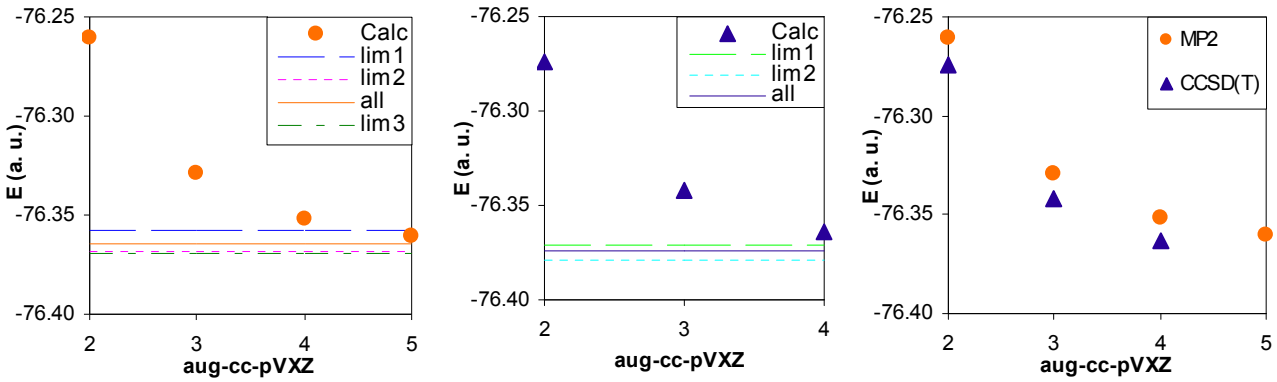

MP2 extrapolations CCSD(T) extrapolations Comparison

Figure 2 Convergence of total electronic energy of water molecule

The three graphs in Figure 2 show the convergence of the total electronic energy of water molecule. Line labeled *lim1* is energy extrapolated utilizing eq. (32), *lim2* CBS energy calculated using eq. (33), and *lim3* corresponds to eq. (34). Label *all* means that all calculated energies were employed in the extrapolation. This labeling is the same in the whole thesis. All these limits are shown, since only values *lim1* are available for larger clusters. It is useful to compare *lim1* with *all*, since it brings information about the extrapolation scheme. So, how correct it is?

The last graph is presented to demonstrate comparison between MP2 and CCSD(T). It shows that the energy difference between these methods is basis set independent, which is why eq. (32) can be used.

5.2. Methanolic clusters

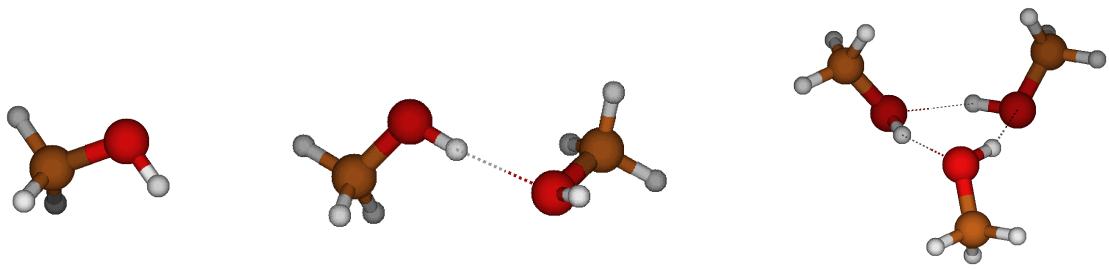

CH_3OH $(CH_3OH)_2$ $(CH_3OH)_3$

Figure 3 Methanolic clusters

Table 2 Bond lengths and angles in $(CH_3OH)_n$

n	1	2		3		
|OH| CH_3OH (Å)	0.961	0.969	-	0.977	0.976	0.977
angle COH CH_3OH (deg)	108.0	107.7	108.4	108.4	108.5	108.5
|OH| H-bond (Å)	-	1.879	-	1.846	1.863	1.841
angle OHO H-bond (deg)	-	168.6	-	152.8	151.9	153.3

Figure 3 shows small methanolic clusters. Methanol forms dimer containing one hydrogen bond and cyclic trimer with three hydrogen bonds. Table 2 provides geometrical properties of investigated methanolic clusters. The length of covalent OH bond of methanol (in the second row) is the distance between oxygen and hydrogen which acts as a donor in hydrogen bond. It gets longer with increasing size of the cluster. Hydrogen bond in methanol dimer (1.88 Å) is shorter than in water dimer (1.95 Å). Hydrogen bond in methanol dimer is longer than in the trimer.

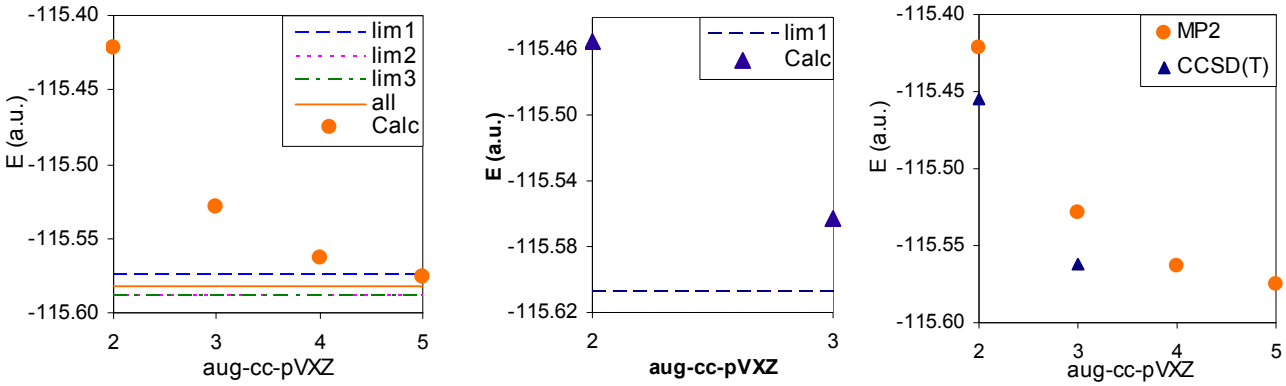

MP2 extrapolations CCSD(T) extrapolations Comparison

Figure 4 Convergence of total electronic energy of methanol molecule

Figure 4 shows dependence of MP2 and CCSD(T) energy of methanol molecules on *X*. It is similar to that of water. The difference between MP2 energy and CCSD(T) energy does not depend on the basis set.

5.3. Clusters containing chloride anion

5.3.1. Structure

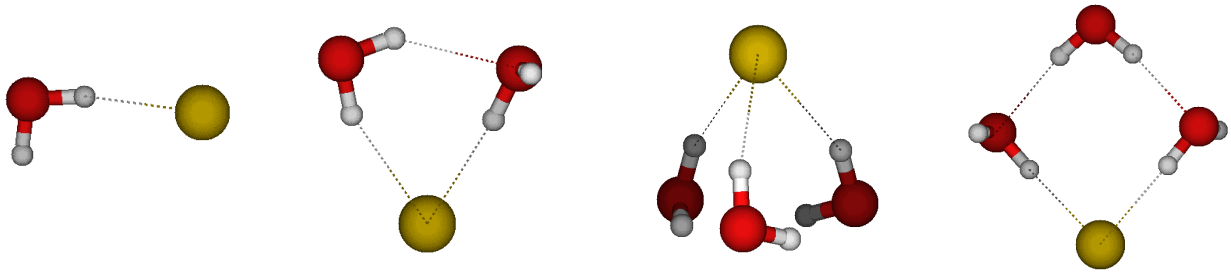

$Cl^-(H_2O)$ $Cl^-(H_2O)_2$ $Cl^-(H_2O)_3$ $Cl^-(H_2O)_{2+1}$

Figure 5 Chloride water clusters

Table 3 Bond lengths and angles in $Cl^-(H_2O)_n$

n	1	2		3			2+1	
|OH| water (Å)	0.991	0.978	0.992	0.979	0.979	0.979	0.990	0.972
|HCl| (Å)	2.118	2.296	2.096	2.267	2.261	2.271	2.096	-
angle OHCl (deg)	168.2	155.9	168.2	154.4	155.0	154.2	170.8	-
angle HClH (deg)	-	67.5		68.0	68.1	68.1	85.4	-

Calculated structures of small chloride-water clusters can be seen in Figure 5, Table 3 refers to corresponding geometrical properties. The optimal geometry of $Cl^-(H_2O)$ is asymmetric (C_s symmetry). A structure of symmetric transition state is also mentioned in the literature[7-9]. The optimal geometry of the n = 2 cluster resembles a cyclic structure which retains a degree of hydrogen bonding between the two water molecules. The optimal geometry of $Cl^-(H_2O)_3$ is pyramidal with all waters almost equivalent. Each water molecule donates one hydrogen to the base of the pyramid and other to Cl^-. The last picture shows stable structure which can be formed from chloride anion and three water molecules, which is a local minimum on potential energy surface. This ring isomer consists of two water molecules binding to the anion (each has one free hydrogen) with the third forming a second solvation shell. The length of covalent OH bond of water is shorter for isolated molecule than that in clusters and is getting shorter with increasing n. In cyclic trimer of water, the OH bond length (0.975 Å) is very close to that OH, hydrogen of which points to chloride, in pyramidal $Cl^-(H_2O)_3$ (0.979 Å).

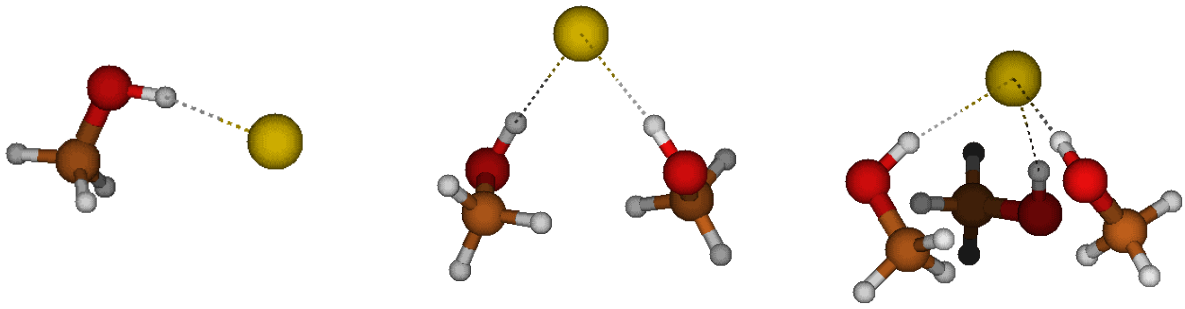

$Cl^-(CH_3OH)$ $Cl^-(CH_3OH)_2$ $Cl^-(CH_3OH)_3$

Figure 6 Chloride methanol clusters

Table 4 Bond lengths and angles in $Cl^-(CH_3OH)_n$

n	1	2		3		
|OH| CH_3OH (Å)	0.992	0.986	0.986	0.981	0.982	0.980
|HCl| (Å)	2.066	2.110	2.110	2.154	2.134	2.160
angle OHCl (deg)	167.7	167.5	167.5	165.7	168.4	166.9
angle HClH (deg)	-	83.2		90.5	81.0	88.9

Optimal structures of chloride-methanol clusters are shown in Figure 6, geometrical properties are provided in Table 4. The optimal structure of $Cl^-(CH_3OH)$ is similar to its water analogue. The hydrogen bond $H\cdots Cl^-$ is shorter in methanol (2.066 Å) than in water (2.118 Å) cluster. From this one can deduce that interaction between chloride and methanol is stronger than between chloride and water. Methanol molecules in $Cl^-(CH_3OH)_2$ are equivalent due to the fact that methanol molecules do not have capability to form solvent-solvent hydrogen bond (unlike water). Structure of $Cl^-(CH_3OH)_3$ is pyramidal and the ionic hydrogen bond HCl is shorter for methanol than for water clusters.

5.3.2. Interaction energy

This part is focused on energetic properties of clusters introduced above. First, we present electronic and association energies of both chloride-water and chloride-methanol cluster. Then tables of calculated energies for cluster of n = 1-3 are shown. Finally comparison between water and methanol is provided.

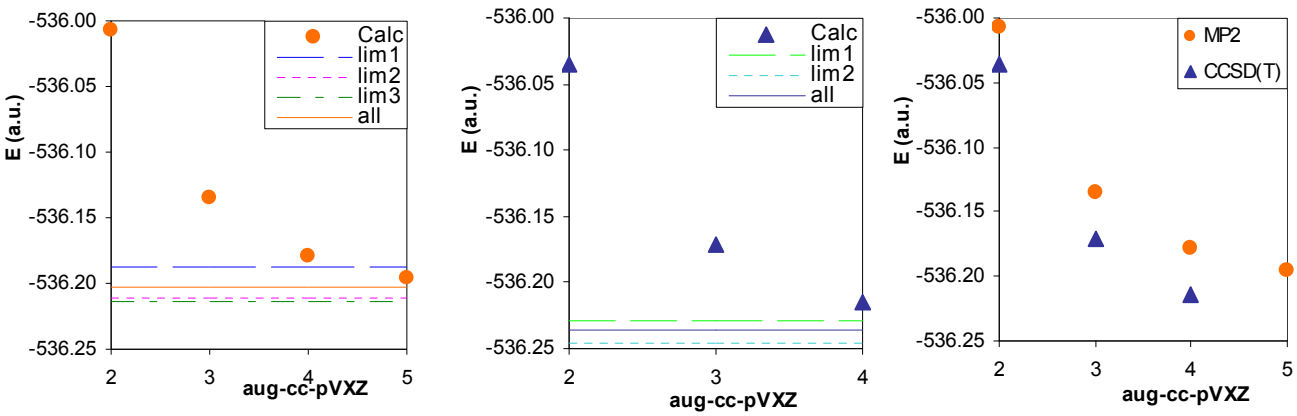

MP2 extrapolations CCSD(T) extrapolations Comparison

Figure 7 Convergence of total electronic energy of $Cl^-(H_2O)$ cluster

Figure 7 illustrates the same features as Figures 2 and 4. Dependence of energy on *X* is similar as before. Value of *lim1* is slightly higher than *all*, the same fact could be seen also for water and methanol. CCSD(T) values of total electronic energy are lower than MP2 values. The difference between MP2 energy and CCSD(T) practically does not change with increasing basis set.

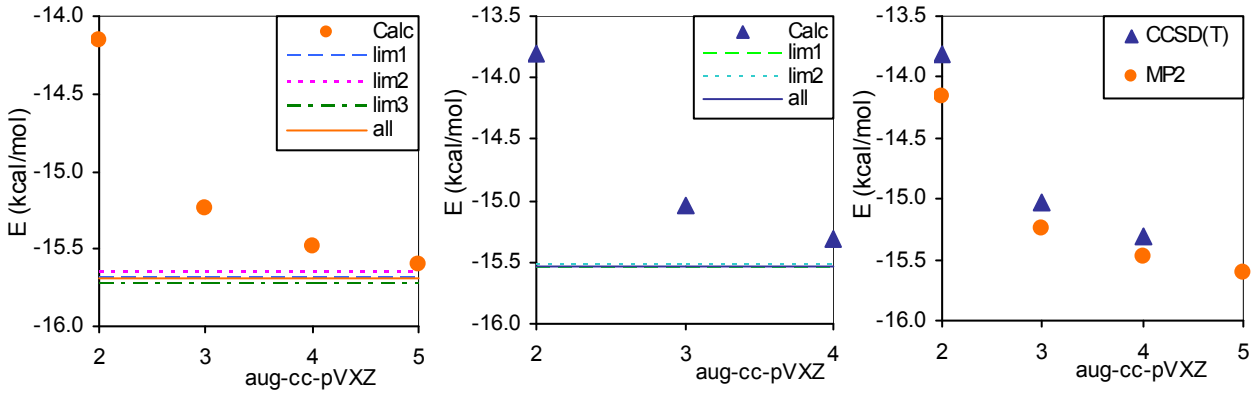

MP2 extrapolations CCSD(T) extrapolations Comparison

Figure 8 Dependence of vertical association energy of $Cl^-(H_2O)$ cluster on basis set

Figure 8 shows dependence of vertical association energy on basis set. It has the same form as that of the total electronic energy. This is understandable, since vertical association energy is the difference of energies of the complex and fragments, which have the same geometry in complex and in isolated form. Value of lim1 almost coincides with all. CCSD(T) values of total electronic energy are slightly higher than MP2 values. The difference between CCSD(T) and MP2 association energy slightly decreases with increasing X.

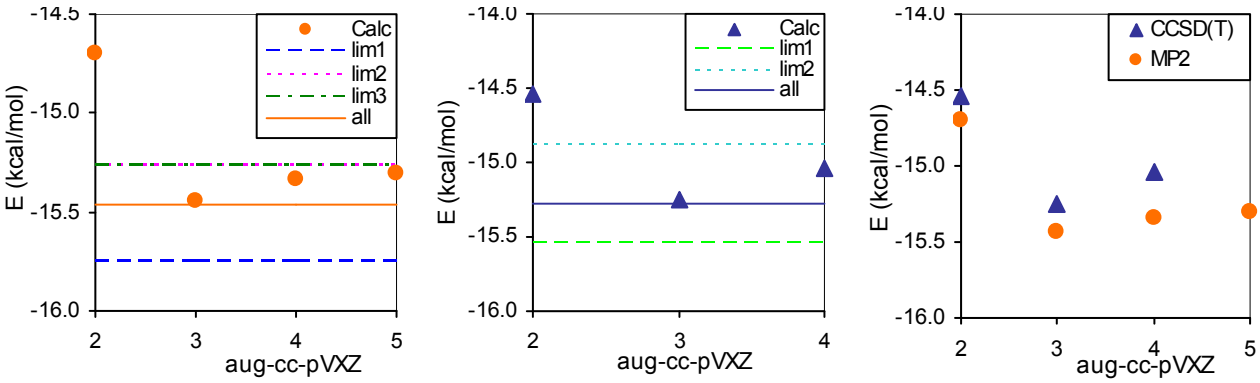

MP2 extrapolations CCSD(T) extrapolations Comparison

Figure 9 Dependence of adiabatic association energy of $Cl^-(H_2O)$ cluster on basis set

Values of adiabatic association energies presented in Figure 9 are not ZPVE corrected. Behavior of adiabatic association energy is not as regular as behavior of vertical association energy. One reason can be that geometry of water in a complex is different from that in a cluster, and dependence of relaxation energy on the cardinal number *X* was not taken into account. Other explanation could be that difference between two monotonously decreasing functions does not have to be a monotonously decreasing function. Nevertheless, the differences between individual limits are smaller than 0.5 kcal/mol, which is not a large error. Value of *lim1* lies lower than *all*, this order was different for vertical energy.

Table 5 Comparison of association energies (in kcal/mol) calculated using the same extrapolation scheme as for larger clusters (eq. 32, 33) and extrapolation employing all points. Adiabatic association energies are ZPVE corrected.

	MP2		CCSD(T)	
	scheme	all	scheme	all
vertical	-15.69	-15.69	-15.34	-15.53
adiabatic	-14.58	-14.29	-14.42	-14.10

Differences between values obtained by a standard extrapolation employing all points and by extrapolation scheme are smaller than 0.3 kcal/mol, which is less than 1 kcal/mol. This value is sometimes called the chemical accuracy.

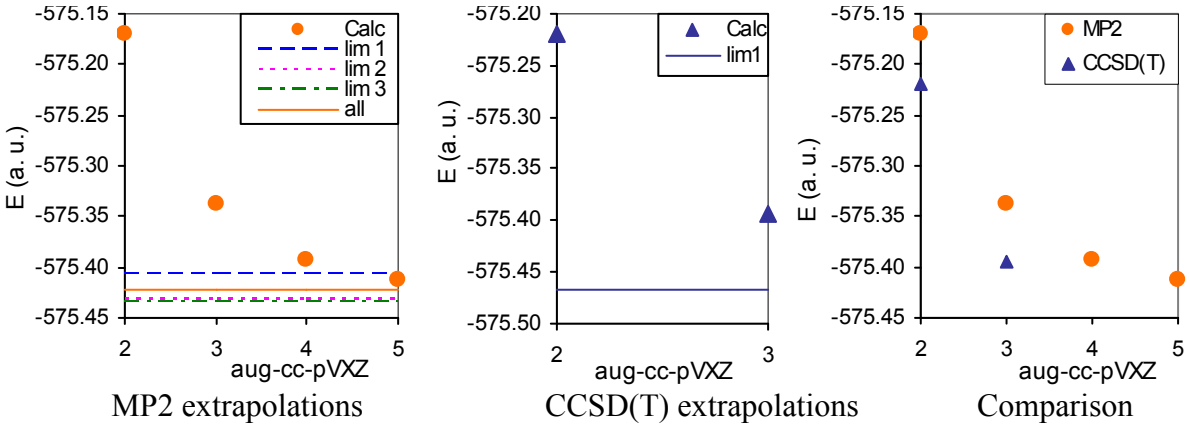

Figure 10 Convergence of total electronic energy of $Cl^-(CH_3OH)$ cluster

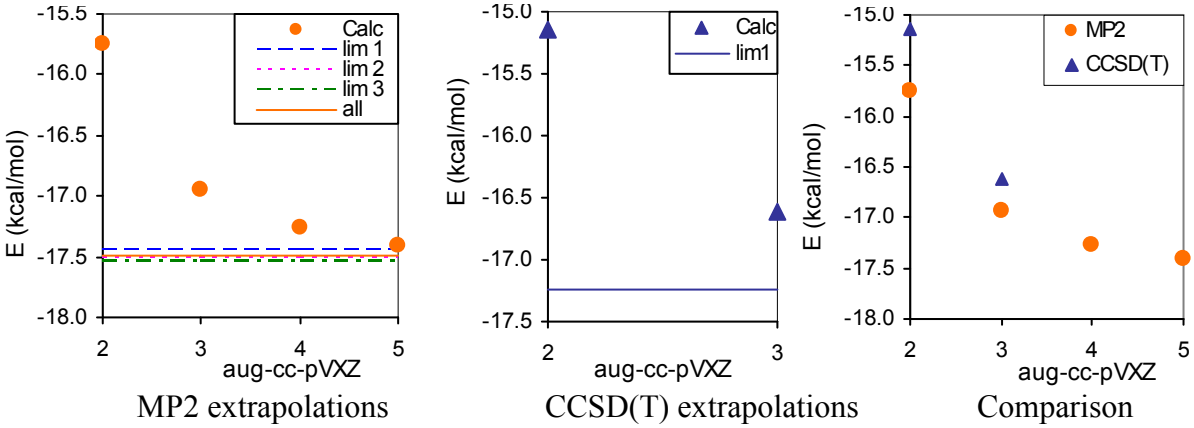

Figure 11 Dependence of vertical association energy of $Cl^-(CH_3OH)$ cluster on basis set

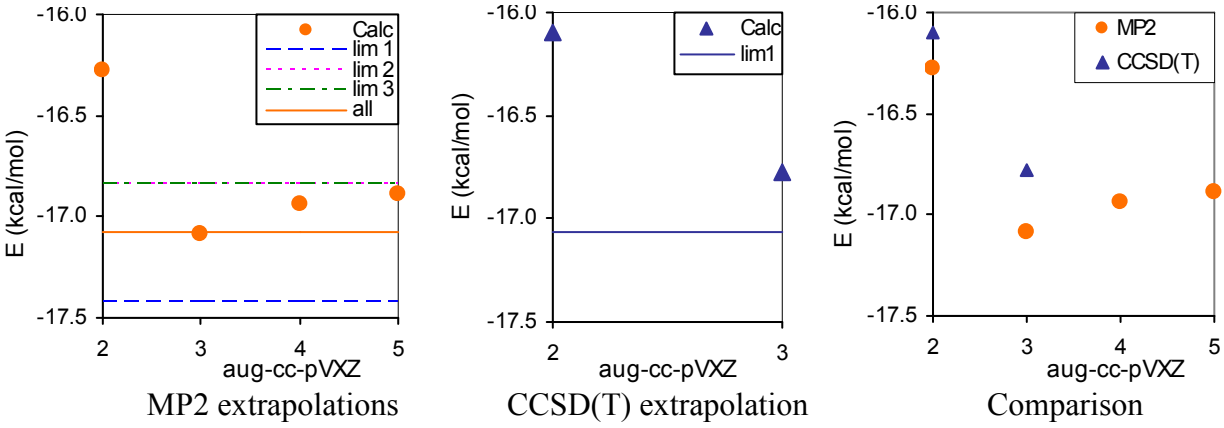

Figure 12 Dependence of adiabatic association energy of $Cl^-(CH_3OH)$ cluster on basis set

Figure 10 illustrates that total electronic energy of $Cl^-(CH_3OH)$ cluster converges to the basis set limit according to employed extrapolation schemes. Values of adiabatic association energies presented in Figure 12 are not ZPVE corrected. Figures 11 and 12 are very similar to Figures 8 and 9, therefore conclusion about convergence of vertical and

adiabatic association energies does not differ from what was written about chloride-water cluster.

Table 6 Comparison of association energies (in kcal/mol) calculated using the same extrapolation scheme as for larger clusters (eq. 32, 33) and extrapolation employing all points. Adiabatic association energies are ZPVE corrected.

	MP2		CCSD(T)	
	scheme	all	scheme	all
vertical	-17.44	-17.49	-16.83	-17.24
adiabatic	-16.94	-16.59	-16.77	-16.58

Table 6 shows that differences between values obtained by extrapolation employing all points and by standard extrapolation scheme are smaller than 0.3 kcal/mol, which is less than chemical accuracy.

Table 7 Vertical and adiabatic association energy of water molecule in kcal/mol

	vertical				adiabatic			
n	MP2/DZ	MP2/TZ	CCSD(T)/DZ	CCSD(T)/CBS	MP2/DZ	MP2/TZ	CCSD(T)/DZ	CCSD(T)/CBS
1	-14.16	-15.24	-13.81	-15.53	-13.74	-14.26	-13.37	-14.10
2	-14.35	-15.25	-14.25	-15.52	-12.78	-13.05	-12.90	-13.28
	-14.53	-15.46	-14.23	-15.55				
3	-15.51	-16.60	-15.41	-16.95	-13.07	13.25	13.69	-13.61
	-15.50	-16.58	-15.40	-16.94				
	-15.49	-16.56	-15.40	-16.93				
2+1	-14.99	-15.72	-14.91	-15.96	-11.51	-11.61	11.50	-11.57
	-14.53	-15.89	-14.19	-16.13				

Table 8 Vertical and adiabatic association energy of ion in $Cl^-(H_2O)_n$ cluster in kcal/mol

	vertical				adiabatic			
n	MP2/DZ	MP2/TZ	CCSD(T)/DZ	CCSD(T)/CBS	MP2/DZ	MP2/TZ	CCSD(T)/DZ	CCSD(T)/CBS
1	-14.16	-15.24	-13.81	-15.53	-13.74	-14.26	-13.37	-14.10
2	-27.18	-28.85	-26.62	-28.99	-23.08	-24.23	-23.09	-24.72
3	-38.49	-40.52	-37.78	-40.66	-28.36	-29.70	-26.48	-28.39
2+1	-36.50	-38.58	-35.70	-38.65	-26.80	-28.06	-24.57	-26.35

Table 9 Vertical and adiabatic association energy of methanol molecule in kcal/mol

	vertical				adiabatic			
n	MP2/DZ	MP2/TZ	CCSD(T)/DZ	CCSD(T)/CBS	MP2/DZ	MP2/TZ	CCSD(T)/DZ	CCSD(T)/CBS
1	-15.75	-16.94	-15.14	-17.24	-15.79	-16.60	-15.62	-16.58
2	-14.41	-15.52	-14.07	-15.65	-15.48	-15.02	-15.82	-15.16
3	-13.09	-14.18	-12.83	-14.38	-13.18	-12.64	-13.39	-12.62
	-12.98	-13.98	-12.67	-14.08				
	-12.60	-12.67	-12.34	-13.66				

Table 10 Vertical and adiabatic association energy of ion in $Cl^-(CH_3OH)_n$ cluster in kcal/mol

	vertical				adiabatic			
n	MP2/DZ	MP2/TZ	CCSD(T)/DZ	CCSD(T)/CBS	MP2/DZ	MP2/TZ	CCSD(T)/DZ	CCSD(T)/CBS
1	-15.75	-16.94	-15.14	-17.24	-15.79	-16.60	-15.62	-16.58
2	-29.60	-31.45	-28.84	-31.48	-25.63	-26.69	-25.50	-27.01
3	-42.00	-44.33	-40.92	-44.24	-28.22	-29.13	-28.24	-29.54

Tables 7 - 10 summarize vertical and adiabatic association energies of solvent and ion in clusters of formula $Cl^-(Solvent)_n$. They contain calculated and extrapolated values of evaluated energies. DZ, and TZ are abbreviations for aug-cc-pVDZ and aug-cc-pVTZ basis sets; adiabatic energies are ZPVE corrected. Values calculated for structure $Cl^-(H_2O)_{2+1}$ show that solvent molecule as well as chloride are bound more weakly than in corresponding global minimum structure, which is due to lower number of hydrogen bonds, that are formed in this cluster.

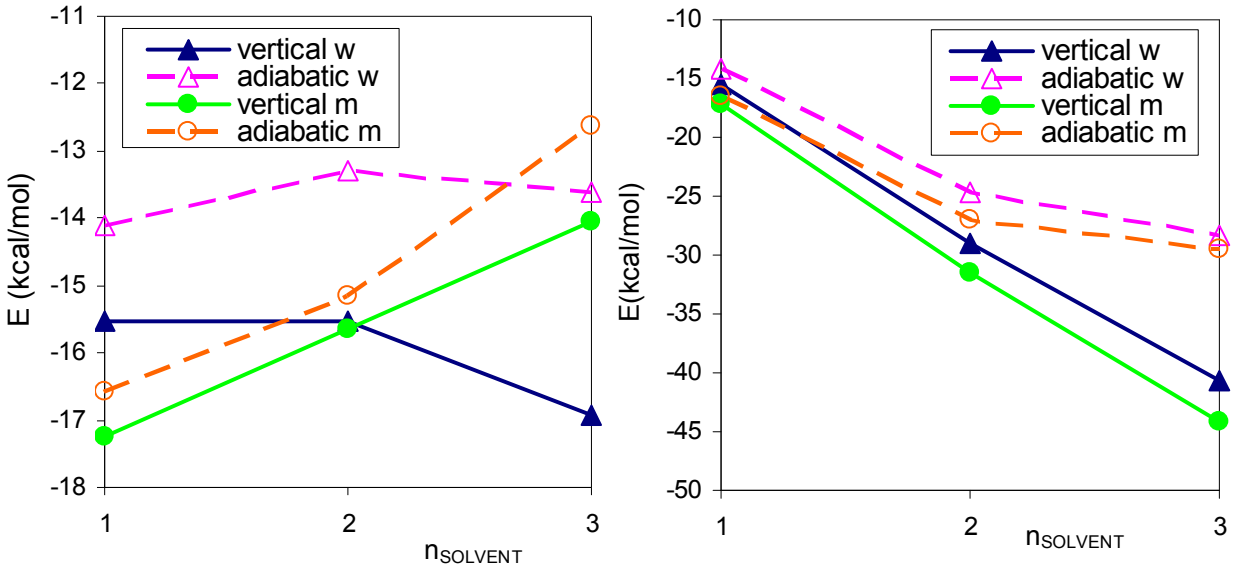

Solvent Ion

Figure 13 Dependence of CCSD(T)/CBS values of association energy on number of solvent molecules in the cluster (n), m is abbreviation for methanol, w for water

Figure 13 summarizes all investigated association energies. We should mention that vertical association energies of solvent molecules were not exactly the same for each solvent molecule in clusters containing more solvent molecules, so plotted values are averages of these energies.

Vertical binding energy of the first and the second water molecule is almost the same. The third molecule is bound more strongly, which was not observed for any other studied

system. Adiabatic binding of the second water molecule is weaker than for the first molecule, the third molecule is bound more strongly than the third molecule. This is probably due to the hydrogen bonding network between water molecules. Vertical and adiabatic binding of methanol decreases with number of solvent molecules. For clusters containing one solvent molecule, binding is stronger in case of methanol. The difference between vertical binding of methanol and water became smaller for cluster containing two solvent molecules. In case of three solvent molecules, the order of methanol and water is reversed.

The strength of vertical ion binding increases almost linearly for both studies and interaction of chloride anion with methanol is stronger than with water. Curves of adiabatic association energies are less straightforward, because reorganization of remaining solvent molecules after removal of ion comes into play. Chloride is bound more strongly in methanolic cluster, but the difference from water for n = 3 almost diminishes in the adiabatic case.

5.4. Clusters containing fluoride anion

5.4.1. Structure

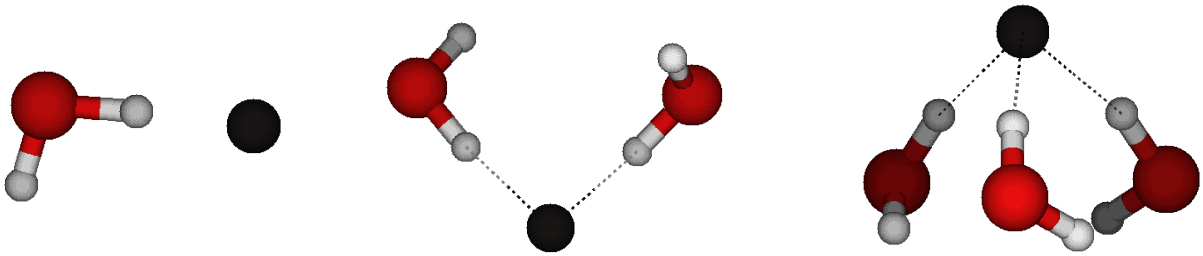

$F^-(H_2O)$ $F^-(H_2O)_2$ $F^-(H_2O)_3$

Figure 14 Fluoride water clusters

Table 11 Bond lengths and angles in $F^-(H_2O)_n$

n	1	2		3		
|OH| water (Å)	1.065	1.021	1.016	0.996	0.996	0.996
|HF| (Å)	1.368	1.516	1.541	1.626	1.626	1.626
OHF (deg)	177.4	174.5	172.8	165.2	165.2	165.2
HFH (deg)	-	95.8		84.2	84.2	84.2

Calculated structures of small fluoride-water clusters can be seen in Figure 14, Table 11 refers to corresponding geometrical properties. Optimized geometries of fluoride water clusters are similar to these of chloride water clusters. The distance between halide and hydrogen is shorter in case of fluoride, for example in clusters containing one solvent molecule, the length of $H\cdots X^-$ hydrogen bond is 2.118 Å in case of chloride and 1.368 Å in case of fluoride. $F^-(H_2O)_2$ is slightly different from $Cl^-(H_2O)_2$, separation between water molecules is larger, so there seems to be a very week interaction between hydrogen of the first water and oxygen of the second water. Larger separation of water molecules in cluster containing fluoride also occurs for n = 3.

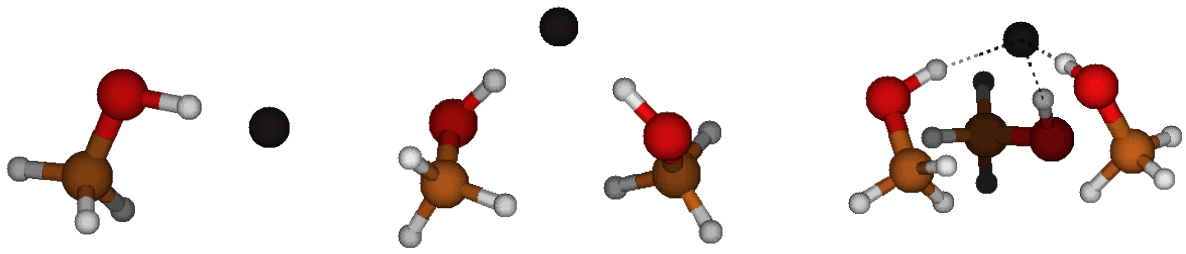

$F^-(CH_3OH)$ $F^-(CH_3OH)_2$ $F^-(CH_3OH)_3$

Figure 15 Fluoride methanol clusters

Table 12 Bond lengths and angles in $F^-(CH_3OH)_n$

n	1	2		3		
|OH| (Å)	1.074	1.016	1.016	0.996	0.997	0.998
|HF| (Å)	1.329	1.490	1.490	1.584	1.581	1.579
angle OHF (deg)	176.1	172.7	172.7	169.6	170.9	173.0
angle HFH (deg)	-	102.0		104.4	106.6	97.1

Figure 15 shows optimized structures of fluoride-methanol clusters, Table 12 provides geometrical properties of these systems. Optimized structures of fluoride methanol clusters are again similar to its chloride analogues. Halide hydrogen distance is shorter and angle HXH is larger than in the chloride case. Ionic hydrogen bond $H\cdots F^-$ in cluster containing one solvent molecule is shorter for methanol (1.329 Å) than for water (1.368 Å). One can thus deduce that interaction between fluoride and methanol will be stronger than between fluoride and water.

5.4.2. Interaction energy

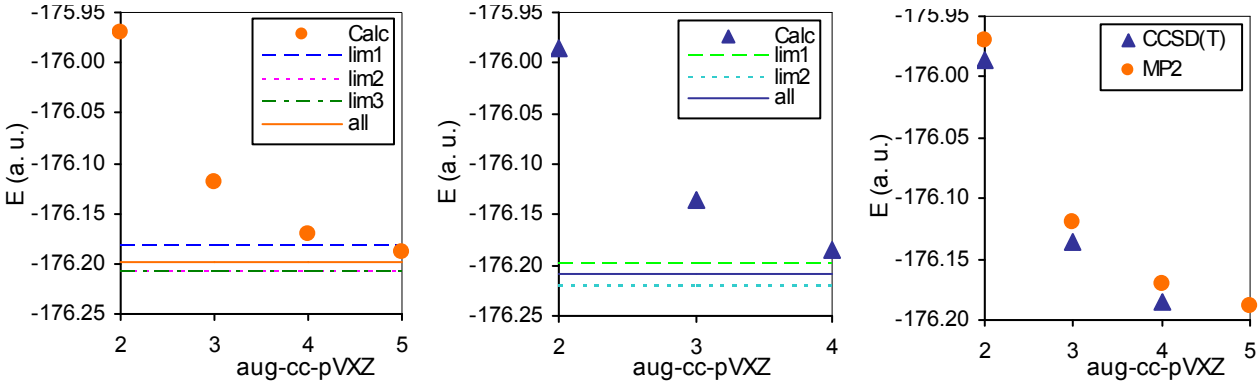

MP2 extrapolations CCSD(T) extrapolations Comparison

Figure 16 Convergence of total electronic energy of $F^-(H_2O)$ cluster

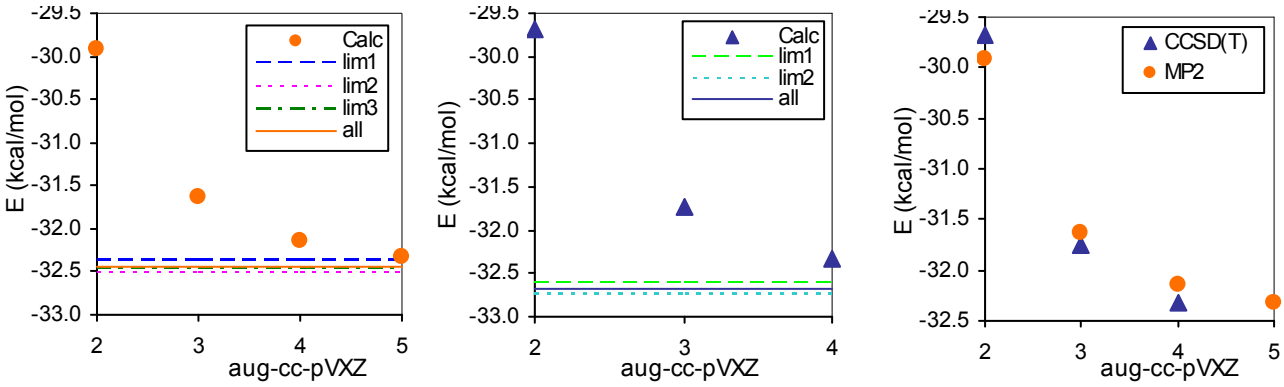

MP2 extrapolations CCSD(T) extrapolations Comparison

Figure 17 Dependence of vertical association energy of $F^-(H_2O)$ cluster on basis set

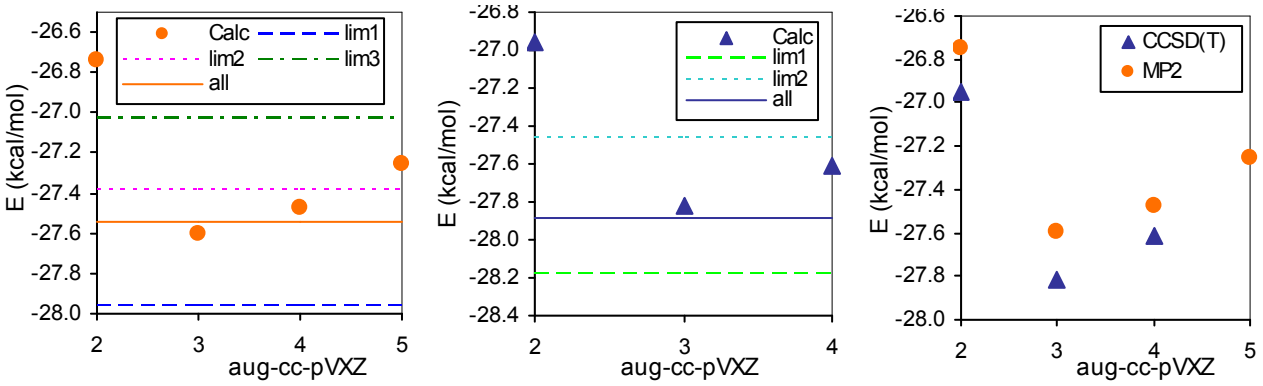

MP2 extrapolations CCSD(T) extrapolations Comparison

Figure 18 Dependence of adiabatic association energy of $F^-(H_2O)$ cluster on basis set

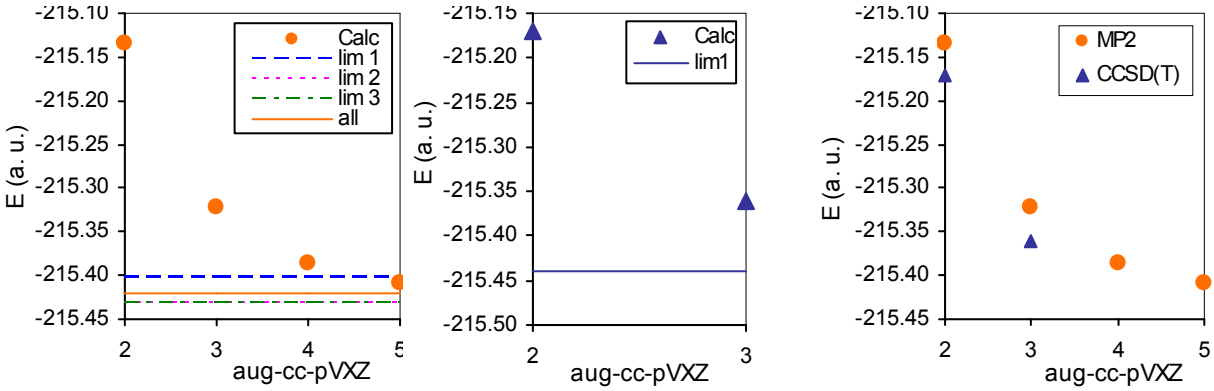

MP2 extrapolations CCSD(T) extrapolations Comparison

Figure 19 Convergence of total electronic energy of $F^-(CH_3OH)$ cluster

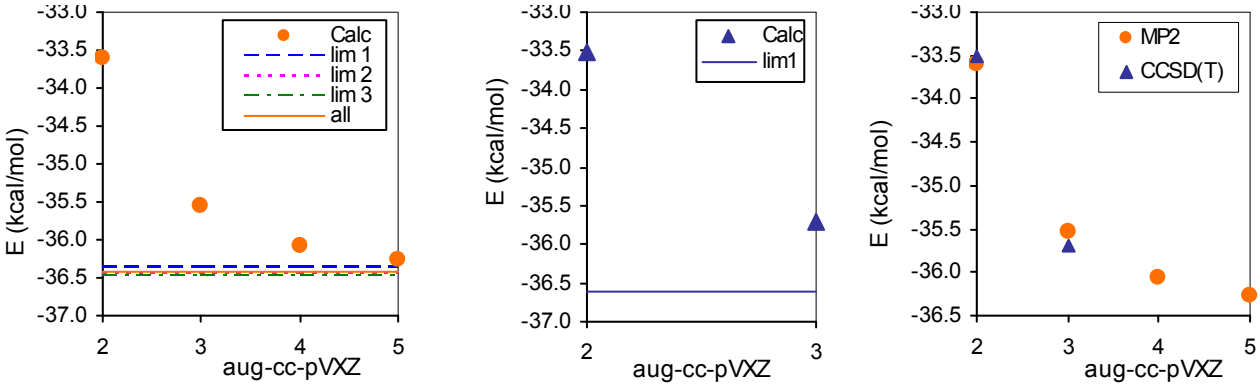

MP2 extrapolations CCSD(T) extrapolations Comparison

Figure 20 Dependence of vertical association energy of $F^-(CH_3OH)$ cluster on basis set

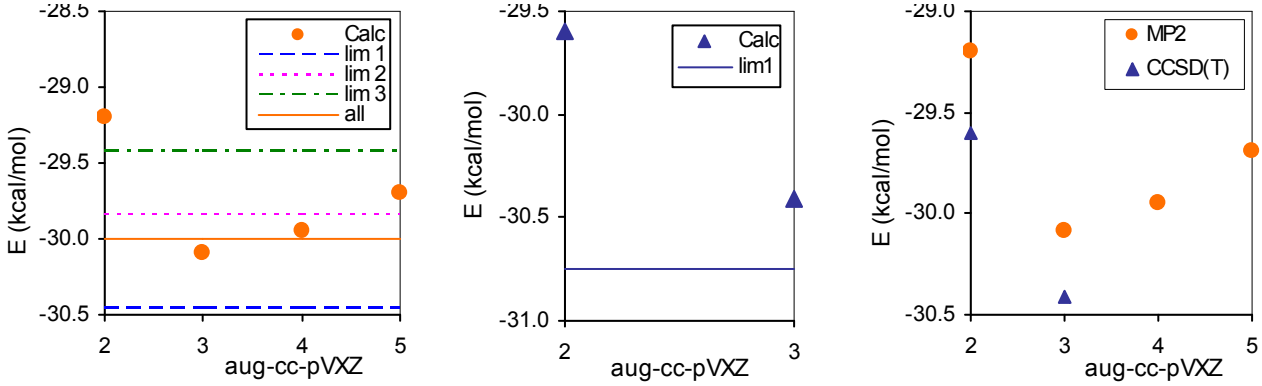

MP2 extrapolations CCSD(T) extrapolations Comparison

Figure 21 Dependence of adiabatic association energy of $F^-(CH_3OH)$ cluster on basis set

Figure 16 depicts analogous results as Figure 7. As can be seen again, *lim1* lies again slightly higher than *all*. Difference between CCSD(T) and MP2 results is basis set independent. Figure 17 shows that the vertical association energy converges to the basis set limit, and results of several extrapolation are very close to each other. Difference between CCSD(T) and MP2 values is positive for aug-cc-pVDZ basis, but negative for larger basis sets. Values of adiabatic association energies presented in Figure 18 are not ZPVE corrected The dependence of adiabatic association energy on *X* is not a monotonously decreasing function, the same behavior can be seen in Figures 9 and 12.

Figure 19 illustrates that total electronic energy of the $F^-(CH_3OH)$ cluster converges to the basis limit according to employed extrapolation schemes. Values of adiabatic association energies presented in Figure 21 are not ZPVE corrected. Figures 20 and 21 are very similar to Figures17 and 18, therefore conclusion about convergence of vertical and adiabatic association energies does not differ from what was written about fluoride-water clusters.

Table 13 Comparison of association energies (in kcal/mol) calculated using the same extrapolation scheme as for larger clusters (eq. 32, 33) and extrapolation employing all points. Adiabatic association energies are ZPVE corrected.

	MP2		CCSD(T)	
	scheme	all	scheme	all
vertical	-32.36	-32.45	-32.12	-32.67
adiabatic	-27.34	-26.92	-27.55	-27.27

Table 14 Comparison of association energies (in kcal/mol) calculated using the same extrapolation scheme as for larger clusters (eq. 32, 33) and extrapolation employing all points. Adiabatic association energies are ZPVE corrected.

	MP2		CCSD(T)	
	scheme	all	scheme	all
vertical	-36.36	-36.42	-36.27	-36.62
adiabatic	-31.02	-30.56	-31.42	-31.31

Table 13 and Table 14 provides that differences between values obtained by extrapolation employing all points and by a standard extrapolation scheme are smaller than 0.5 kcal/mol, which is less than chemical accuracy.

Table 15 Vertical and adiabatic association energy of water molecule in kcal/mol

	vertical				adiabatic			
n	MP2/DZ	MP2/TZ	CCSD(T)/DZ	CCSD(T)/CBS	MP2/DZ	MP2/TZ	CCSD(T)/DZ	CCSD(T)/CBS
1	-29.92	-31.64	-29.68	-32.67	-26.13	-26.98	-26.34	-27.27
2	-21.57	-22.62	-21.60	-23.09	-18.49	-18.26	-18.93	-18.59
	-21.92	-23.04	-21.91	-23.50				
3	-18.58	-19.53	-18.75	-20.10	-15.71	-15.58	-16.32	-16.13

Table 16 Vertical and adiabatic association energy of ion in $F^-(H_2O)_n$ cluster in kcal/mol

	vertical				adiabatic			
n	MP2/DZ	MP2/TZ	CCSD(T)/DZ	CCSD(T)/CBS	MP2/DZ	MP2/TZ	CCSD(T)/DZ	CCSD(T)/CBS
1	-29.92	-31.64	-29.68	-32.67	-26.13	-26.98	-26.34	-27.27
2	-49.16	-51.23	-49.10	-52.04	-41.40	-42.15	-42.09	-43.16
3	-65.17	-66.98	-65.18	-67.75	-49.33	-49.95	-50.66	-51.55

Table 17 Vertical and adiabatic association energy of methanol molecule in kcal/mol

	vertical				adiabatic			
n	MP2/DZ	MP2/TZ	CCSD(T)/DZ	CCSD(T)/CBS	MP2/DZ	MP2/TZ	CCSD(T)/DZ	CCSD(T)/CBS
1	-33.60	-35.54	-33.51	-36.42	-29.76	-30.65	-30.16	-31.31
2	-23.09	-24.17	-23.16	-24.68	-21.45	-20.52	-22.29	-20.96
3	-18.38	-19.28	-18.53	-19.80	-16.89	-16.04	-17.54	-16.33
	-18.25	-19.13	-18.34	-19.59				
	-17.92	-18.75	-18.07	-19.24				

Table 18 Vertical and adiabatic association energy of ion in $F^-(CH_3OH)_n$ cluster in kcal/mol

	vertical				adiabatic			
n	MP2/DZ	MP2/TZ	CCSD(T)/DZ	CCSD(T)/CBS	MP2/DZ	MP2/TZ	CCSD(T)/DZ	CCSD(T)/CBS
1	-33.60	-35.54	-33.51	-36.42	-29.76	-30.65	-30.16	-31.31
2	-52.22	-54.30	-52.36	-55.32	-45.57	-46.24	-46.52	-47.47
3	-68.67	-70.94	-68.94	-72.15	-51.88	-52.09	-53.41	-53.70

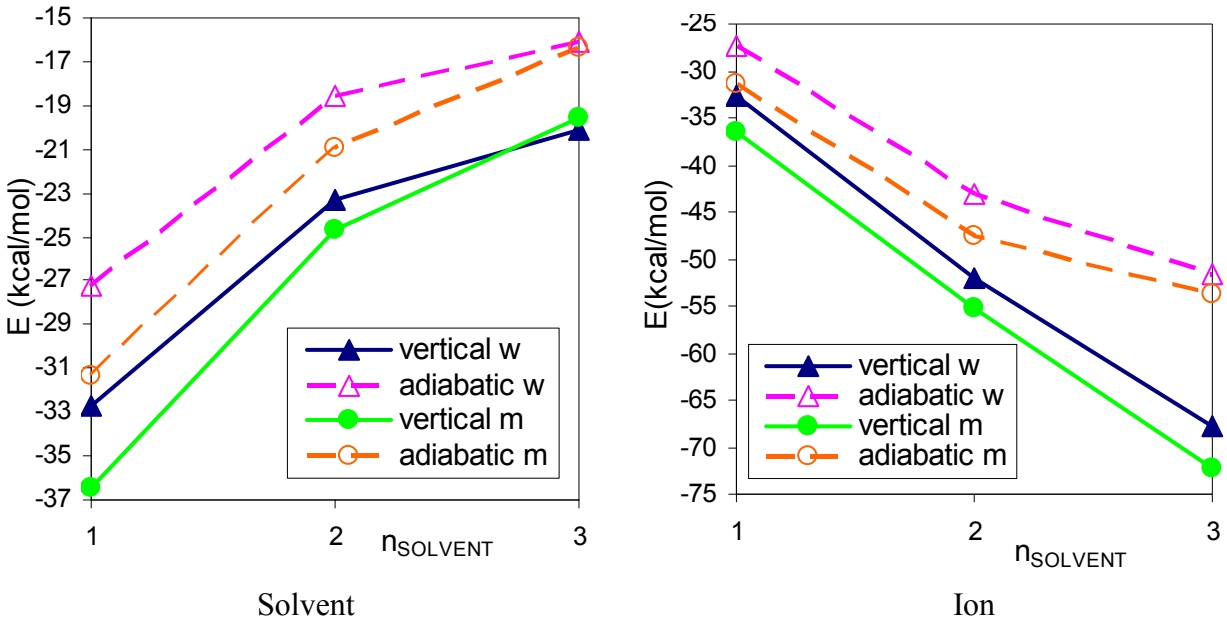

Solvent Ion

Figure 22 Dependence of CCSD(T)/CBS values of association energy on number of solvent molecules in the cluster (n), m is abbreviation for methanol, w for water

Figure 22 summarizes all investigated association energies of $F^-(Solvent)_n$ clusters. It should be mentioned that vertical association energies of solvent molecules were not exactly the same for each solvent molecules in clusters containing more solvent molecules, so plotted values are averages of these energies. First we pointed out short comparison with chloride. Although qualitatively the binding pattern is similar to that of chloride, fluoride interacts with solvent molecules more strongly due to its smaller size and, therefore, higher charge density.

Vertical, as well as adiabatic binding decreases with increasing number of solvent molecules. Interaction with methanol is stronger than with water for the smallest clusters. A crossover between water and methanol occurs only for the vertical case, values of vertical association energies of solvent molecule are almost the same for n = 3.

The strength of vertical ion binding increases almost linearly in both cases and interaction of fluoride anion with methanol is stronger than with water. Curves of adiabatic association energies are less straightforward, because reorganization of remaining solvent molecules after removal of ion comes into play. Fluoride is bound more strongly in methanolic cluster, but the difference from water for n = 3 is smaller than in the vertical case.

5.5. Clusters containing sodium cation

5.5.1. Structure

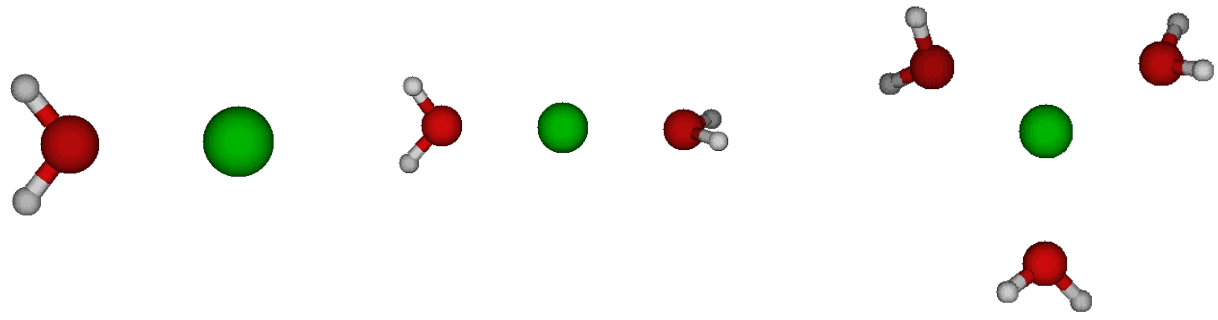

$Na^+(H_2O)$ $Na^+(H_2O)_2$ $Na^+(H_2O)_3$

Figure 23 Sodium water clusters

Table 19 Bond lengths and angles in $Na^+ (H_2O)_n$

n	1	2	3
|OH| (Å)	0.965	0.964	0.964
|NaO| (Å)	2.277	2.306	2.342
angle NaONa(deg)	-	179.5	120.0

Calculated structures of small sodium-water clusters can be seen in Figure 23, Table 19 refers to corresponding geometrical properties. Cations bind differently to solvent molecules than anions. Solvent molecules orient in such a way that the oxygen atom faces the cation as one would deduce from the positive charge of the ion and the electronegative character of oxygen. The $Na^+(H_2O)_2$ complex possesses a linear structure, by which a linear O-Na-O atom sequence is meant. In the cluster of $n = 3$, the three water molecules lie symmetrically around sodium cation, and oxygen atoms form an equilateral triangle. As can be seen in Table 19, the $O\cdots Na^+$ distance increases with increasing number of water molecules. No hydrogen bonds can be formed.

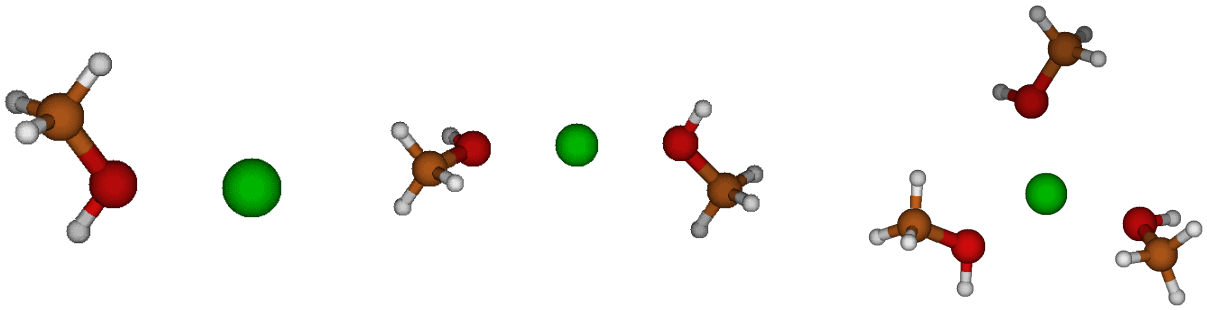

$Na^+(CH_3OH)$ $Na^+(CH_3OH)_2$ $Na^+(CH_3OH)_3$

Figure 24 Sodium methanol clusters

Table 20 Bond lengths and angles in $Na^+ (CH_3OH)_n$

n	1	2	3
OH (Å)	0.964	0.964	0.963
NaO (Å)	2.262	2.293	2.328
angle NaONa (deg)	-	178.8	119.4

Figure 24 shows optimized sodium-methanol clusters, Table 20 provides corresponding geometrical properties of these clusters. Sodium methanol clusters are similar to sodium water clusters. Methanol, as well as water molecules surround central ion to form "interior structures". Structures are similar also due to the absence of hydrogen bonds in water clusters. NaO distance is shorter in methanolic clusters for all n.

5.5.2. Interaction energy

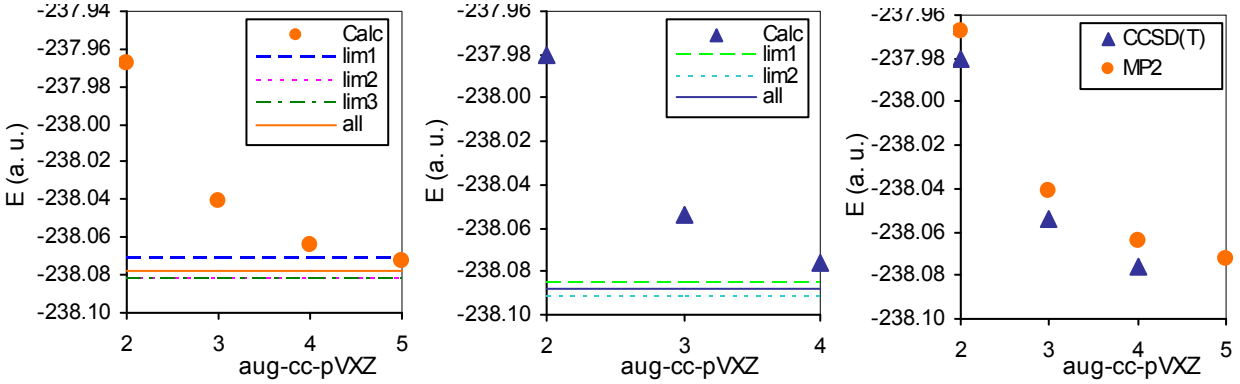

MP2 extrapolations CCSD(T) extrapolations Comparison

Figure 25 Convergence of total electronic energy of $Na^+(H_2O)$ cluster

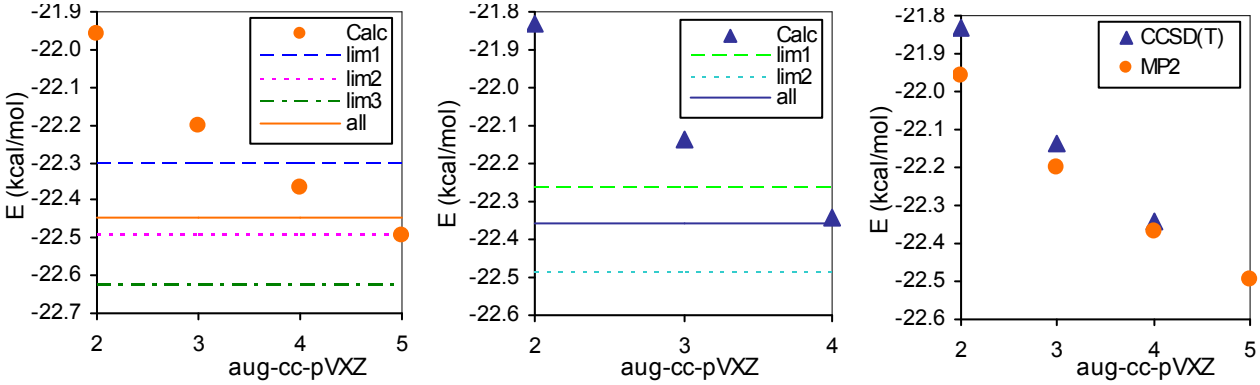

MP2 extrapolations CCSD(T) extrapolations Comparison

Figure 26 Dependence of vertical association energy of $Na^+(H_2O)$ cluster on basis set

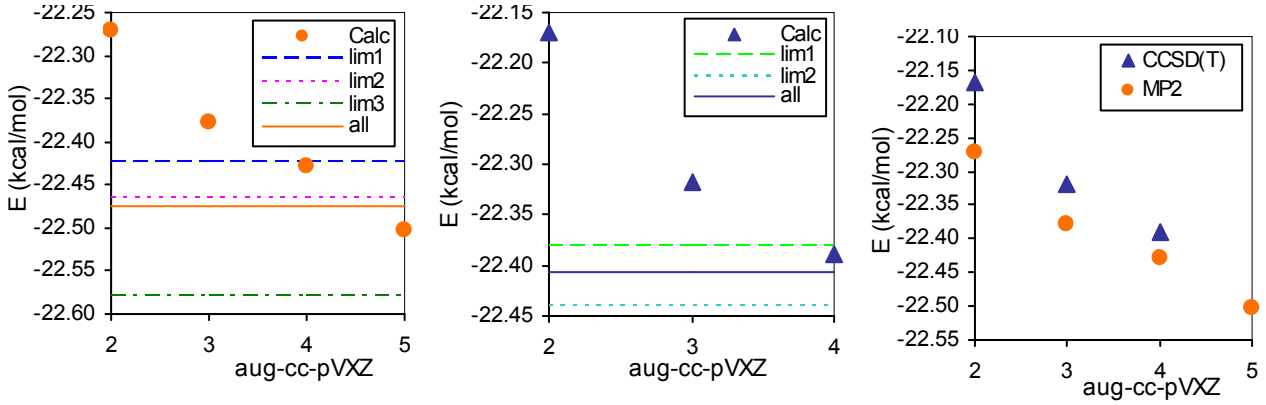

MP2 extrapolations CCSD(T) extrapolations Comparison

Figure 27 Dependence of adiabatic association energy of $Na^+(H_2O)$ cluster on basis set

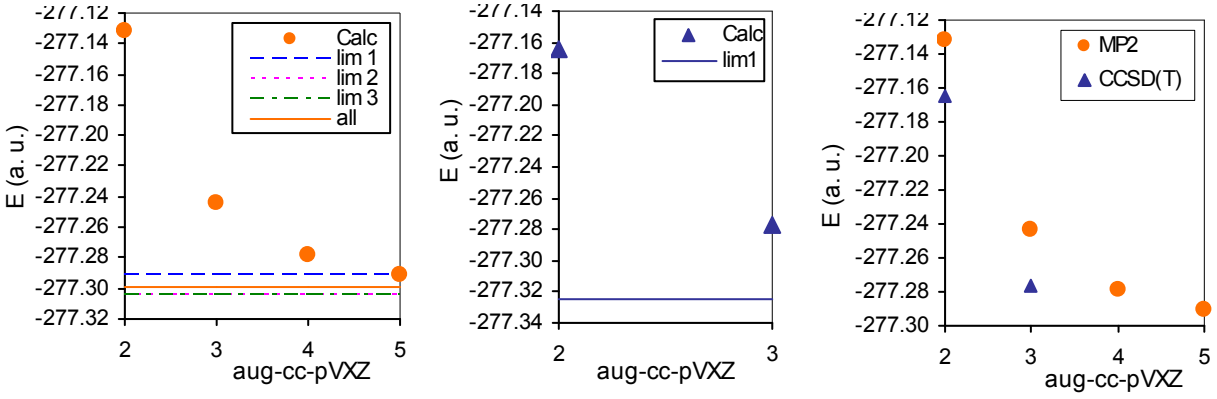

MP2 extrapolations CCSD(T) extrapolations Comparison

Figure 28 Convergence of total electronic energy of $Na^+(CH_3OH)$ cluster

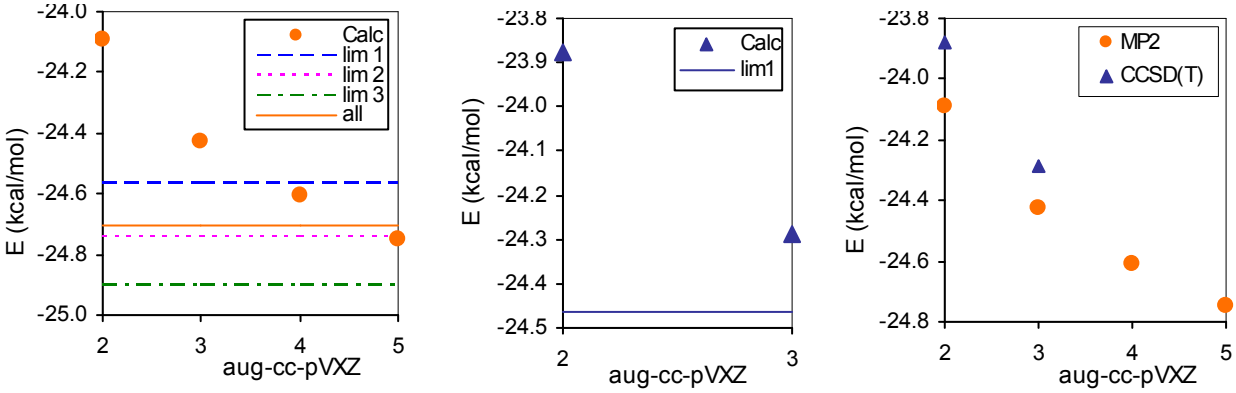

MP2 extrapolations CCSD(T) extrapolations Comparison

Figure 29 Dependence of vertical association energy of $Na^+(CH_3OH)$ cluster on basis set

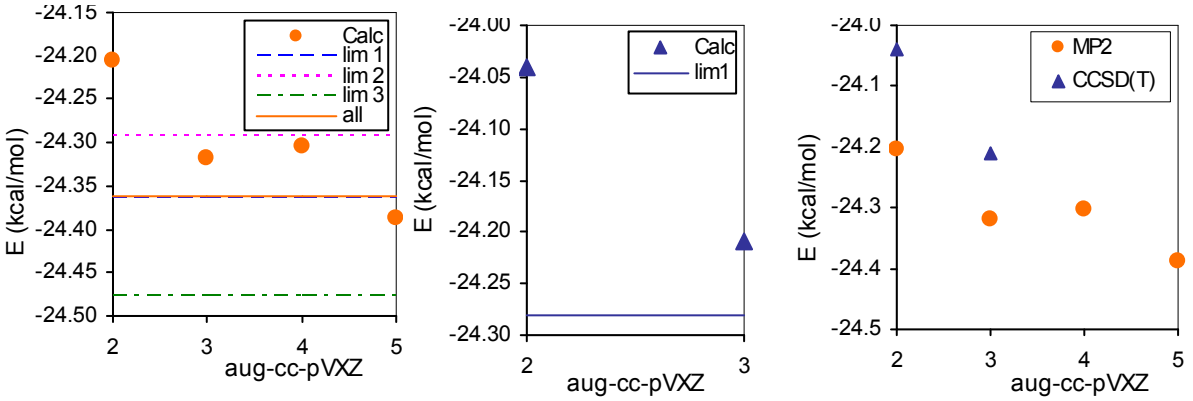

MP2 extrapolations CCSD(T) extrapolations Comparison

Figure 30 Dependence of adiabatic association energy of $Na^+(CH_3OH)$ cluster on basis set

Figure 25 shows that total electronic energy of $Na^+(H_2O)$ converges to the basis set limit according to the presumption, *lim1* lies slightly higher that *all* and difference between CCSD(T) and MP2 energies is basis set independent. As can be seen in Figure 26 vertical association energy of $Na^+(H_2O)$ decreases almost linearly with increasing basis set, although electronic energy of the complex, sodium cation and water molecule calculated employing basis of the complex decreases according to eq. (23). Energy of sodium converges faster to the basis set limit than energy of other components, which can lead to an irregular behavior of vertical association energy. Difference between CCSD(T) and MP2 energy is not basis set independent, but it decreases with increasing *X*.

Figure 28 shows that total electronic energy of $Na^+(CH_3OH)$ converges to the basis set limit, *lim1* lies slightly higher that *all* and difference between CCSD(T) and MP2 energies is basis set independent. Figure 29 shows that that vertical association energy of $Na^+(CH_3OH)$ decreases linearly with increasing basis set, the same picture is shown by Figure 26 for water cluster. Values of adiabatic association energies presented in Figures 27 and 30 are not ZPVE corrected. Adiabatic association energy of $Na^+(H_2O)$ also decreases linearly with increasing *X*. Not only effect of relaxation, but also the fact that electronic energy of sodium cation converges faster than that of other components influence present results. Adiabatic association energy of $Na^+(CH_3OH)$ cluster roughly decreases with increasing *X*.

Table 21 Comparison of association energies (in kcal/mol) calculated using the same extrapolation scheme as for larger clusters (eq. 32, 33) and extrapolation employing all points. Adiabatic association energies are ZPVE corrected.

	MP2		CCSD(T)	
	scheme	all	scheme	all
vertical	-22.30	-22.44	-22.18	-22.36
adiabatic	-20.94	-20.99	-20.84	-20.92

Table 22 Comparison of association energies (in kcal/mol) calculated using the same extrapolation scheme as for larger clusters (eq. 32, 33)and extrapolation employing all points Adiabatic association energies are ZPVE corrected.

	MP2		CCSD(T)	
	scheme	all	scheme	all
vertical	-24.57	-24.71	-24.35	-24.46
adiabatic	-23.30	-23.30	-23.14	-23.22

Differences between values obtained by extrapolation employing all points and by extrapolation scheme are smaller than 0.2 kcal/mol.

Table 23 Vertical and adiabatic association energy of water molecule in kcal/mol

	vertical				adiabatic			
n	MP2/DZ	MP2/TZ	CCSD(T)/DZ	CCSD(T)/CBS	MP2/DZ	MP2/TZ	CCSD(T)/DZ	CCSD(T)/CBS
1	-21.96	-22.20	-21.83	-22.36	-20.79	-20.90	-20.69	-20.92
2	-19.85	-19.94	-19.73	-19.87	-18.91	-18.73	-18.85	-18.59
3	-17.14	-17.14	-17.06	-17.06	-15.48	-15.37	-15.44	-15.29

Table 24 Vertical and adiabatic association energy of ion in $Na^+(H_2O)_n$ cluster in kcal/mol

	vertical				adiabatic			
n	MP2/DZ	MP2/TZ	CCSD(T)/DZ	CCSD(T)/CBS	MP2/DZ	MP2/TZ	CCSD(T)/DZ	CCSD(T)/CBS
1	-21.96	-22.20	-21.83	-22.36	-20.79	-20.90	-20.69	-20.92
2	-42.61	-42.90	-42.35	-42.76	-36.49	-36.54	-36.36	-36.44
3	-61.04	-61.38	-60.69	-61.17	-44.18	-44.14	-44.05	-44.00

Table 25 Vertical and adiabatic association energy of methanol molecule in kcal/mol

	vertical				adiabatic			
n	MP2/DZ	MP2/TZ	CCSD(T)/DZ	CCSD(T)/CBS	MP2/DZ	MP2/TZ	CCSD(T)/DZ	CCSD(T)/CBS
1	-24.09	-24.43	-23.88	-24.46	-23.14	-23.25	-22.98	-23.22
2	-21.42	-21.50	-21.24	-21.35	-21.21	-20.52	-21.37	-20.40
3	-18.10	-18.16	-17.99	-18.04	-16.50	-16.64	-16.19	-16.38

Table 26 Vertical and adiabatic association energy of ion in $Na^+(CH_3OH)_n$ cluster in kcal/mol

	vertical				adiabatic			
n	MP2/DZ	MP2/TZ	CCSD(T)/DZ	CCSD(T)/CBS	MP2/DZ	MP2/TZ	CCSD(T)/DZ	CCSD(T)/CBS
1	-24.09	-24.43	-23.88	-24.46	-23.14	-23.25	-22.98	-23.22
2	-46.37	-46.62	-45.93	-46.29	-38.70	-38.85	-38.41	-38.62
3	-65.05	-65.55	-63.98	-64.69	-44.62	-45.29	-43.95	-43.95

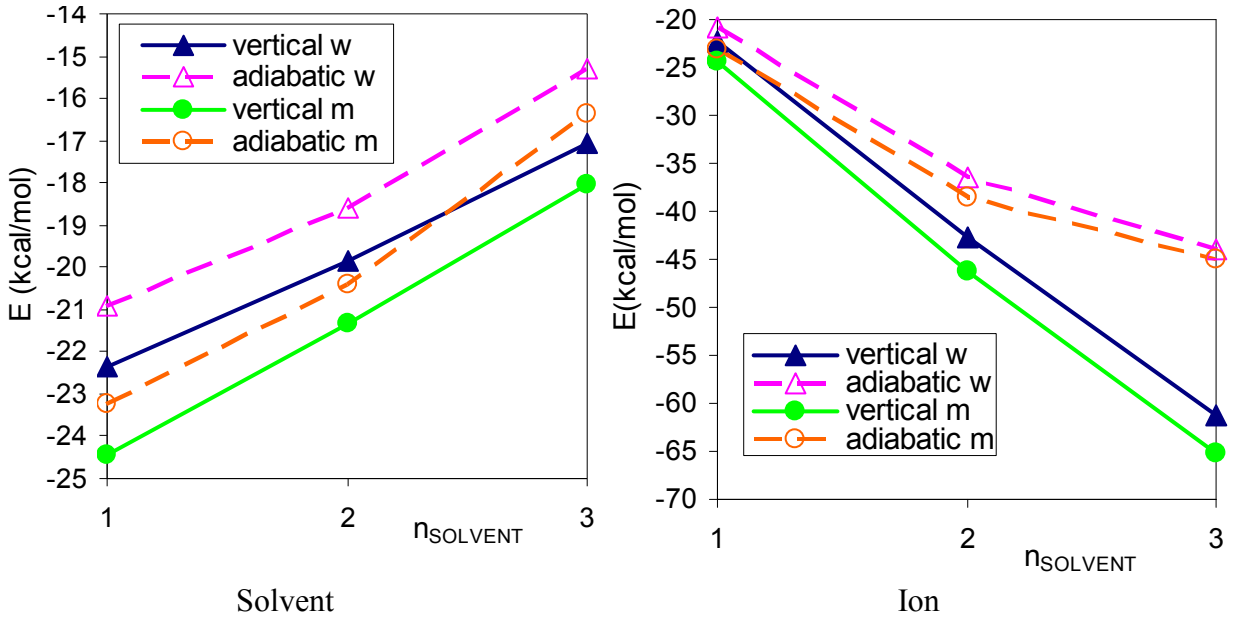

Figure 31 Dependence of CCSD(T)/CBS values of association energy on number of solvent molecules in the cluster (n), m is abbreviation for methanol, w for water

Figure 31 shows the association energies for small sodium-water and sodium-methanol clusters. The binding strength of solvent to sodium lies between those to fluoride and chloride, but closer to the former one. The binding strength of a solvent molecule decreases with increasing cluster size in all case. No crossover of corresponding water and methanol curves occurs.

The strength of vertical binding of sodium in the cluster increases almost linearly, while the behavior of adiabatic binding is less straightforward. Methanol wins as the preferred micro-solvent for sodium over water in all cases. This is due to the fact that the geometry of water-sodium binding does not allow for creating stabilizing water-water hydrogen bonds.

5.6. Comparison with literature

The goal of this section is to discuss the reliability of the results of presented thesis and compare them with experimental results as well as some previous calculations.

Rather surprisingly, for one of the simplest system, namely solvation of fluoride by a single water molecule, there exists a large discrepancy in the 0 K association enthalpy. Reported values range from -23.3 kcal/mol, obtained by previous experiments[16] , to -28 kcal/mol calculated at MP4 level. Bowers and Xantheas reported in their combined

theoretical and experimental study[29] -27.4 ± 0.5 kcal/mol as a result of experiment and -26.5 kcal/mol as a result of CCSD(T) calculation without extrapolation of electronic energy, but with anharmonic correction for ZPVE. These values are in agreement with -27.3 kcal/mol obtained in this work.

Values of association enthalpies extrapolated to values at 0 K are noted in Tables 27 – 32 with references. VAE is the abbreviation of vertical association energy calculated in this thesis and corresponding AAE is the abbreviation of adiabatic association energies. Energies describe this process:

$$\mathrm{Ion(Solvent)_{n-1}} + \mathrm{Solvent} \rightarrow \mathrm{Ion(Solvent)_n}\,. \qquad (35)$$

Table 27 Association energies in chloride-water clusters in kcal/mol

n-1, n	VAE	AAE	[16]	[22] (ZTRID)	[22] (HPMS)	[36] (EFP)	[2]
0, 1	-15.5	-14.1	-13.3			-10.8	14.7
1, 2	-15.5	-13.3	-12.7	-10.1	-10.4	-10.3	13.0
2, 3	-16.9	-13.6	-11.7	-7.2	-9.5	-10.6	11.8

Table 27 shows association energies in chloride-water clusters. Incremental adiabatic association energies are in reasonable agreement with experimental results[2,16], (AAE predicts probably too strong binding of the third water molecule). ZTRID and HPMS techniques probably underestimate the strength of water binding, similarly as calculations employing effective fragment potentials (EFP).

Table 28 Association energies in chloride-methanol clusters in kcal/mol

n-1, n	VAE	AAE	[38] (MP2)	[21]
0, 1	-17.2	-16.6	-16.6	-17.5
1, 2	-15.6	-15.2		-14.1
2, 3	-14.04	-12.6		-11.5

Incremental adiabatic association energies provided in Table 28 are in reasonable agreement with experimental results[21], AAE predicts slightly stronger binding of the second and third methanol molecule. But the differences are within chemical accuracy.

Table 29 Association energies in fluoride-water clusters in kcal/mol

n-1, n	VAE	AAE	[16]	[36] (EFP)	[2]
0, 1	-32.7	-27.3	-23.3	-17.3	
1, 2	-23.3	-18.6	-16.6	-15.3	-19.2
2, 3	-20.1	-16.1	13.7	-14.0	-15.3

The discussion about fluoride water binding which is summarized in Table 29 was already presented in the introduction of this section. AAE values are in agreement with Hiraoka's[2], Arshadi[16] predicts weaker binding, and calculations using EFP predict even weaker binding.

Table 30 Association energies in fluoride-methanol clusters in kcal/mol

n-1, n	VAE	AAE	[38] (MP2)	[38] (PHPMS)	[21]
0, 1	-36.4	-31.3	-30.9	-30.5	
1, 2	-24.7	-21.0			-20.3
2, 3	-19.5	-16.3			-15.1

Only few experimental data about the fluoride methanol interactions were found in the literature as can be seen in Table 30. AAE is in agreement with PHPMS[21,38] results. The difference is smaller than chemical accuracy.

Table 31 Association energies in sodium-water clusters in kcal/mol

n-1, n	VAE	AAE	[15]	[25]	[25]	[25]
0, 1	-22.4	-20.9	-24.0	-22.6	-19.7	-21.0
1, 2	-19.9	-18.6	-19.8			
2, 3	-17.1	-15.3	-15.8			

Table 32 Association energies in sodium-methanol clusters

n-1, n	VAE	AAE	[17]	[23] (epx.)	[23] (MP2)	[25]	[25]	[25]
0, 1	-24.5	-23.2	-26.6	-21.9	-23.8	-21.9	-23.4	-23.2
1, 2	-21.3	-20.4	-20.2					
2, 3	-18.0	-16.4	-17.4					

Table 31 and 32 provide association enthalpies of sodium to water and methanol, resp. Amicangelo[25] studied sodium-solvent clusters using three modifications of CID, which explains why three values are mentioned in these two tables. AAE of one water molecule is in the best agreement with the third modification of CID. Comparison between CID and HPMS[15] indicates that HPMS probably overestimates the strength of binding of water to sodium cation. Other incremental association enthalpies are in agreement with calculations. AAE of one methanol molecule is in the best agreement with the third modification of CID. Results obtained by HPMS[17] probably predict stronger binding of methanol to sodium cation. Adiabatic association energies of methanol molecule for clusters containing more solvent molecules are close to HPMS results.

6. Conclusion

Optimal structures and vertical and adiabatic binding energies of ions and solvent molecules in clusters of sodium, fluoride, or chloride with one to three water and methanol molecules have been presented. These energies are based on CCSD(T) in the complete basis set limit. Extrapolation from the bulk based on Born's model of solvation predicts that water having relative permittivity ε_r = 80 will interact with ions more strongly than methanol having relative permittivity ε_r = 33. However, this extrapolation cannot be directly applied to small clusters investigated this thesis. Namely, in the smallest clusters (containing one solvent molecule) interactions of ions with methanol are stronger than those with water. This fact can be racionalized by ion-dipole, ion-induced dipole model, in which dipole moment of the solvent as well as its polarizability play important role.

The strength of ion or solvent binding in the cluster is determined not only by the nature of ion (mainly the charge density) but also the arrangement of solvent molecules plays an important role. Water unlike methanol can form additional hydrogen bonds in small anion-solvent cluster, which leads to an additional stabilization of the aqueous cluster with more than a single water molecule. To quantify these effects vertical and adiabatic association energies of solvent molecule and ion were calculated. Based on association energies of a solvent molecule, it can be concluded that water becomes a better solvent in clusters with chloride and three solvent molecules, due to the additional hydrogen bonding between water molecules. Water is almost as "good" as methanol in analogous fluoride-solvent cluster. Arrangement of solvent molecules around sodium cation does not allow water molecules to form stabilizing hydrogen bonds, so larger clusters are needed for flipping the preference on the water side. On the other hand vertical association energies of an ion for both cationic and anionic clusters almost linearly decrease with increasing cluster size and ion is bound more strongly in clusters containing methanol in all investigated cases. Also based on adiabatic association energies, methanol is a "better" solvent for clusters of all investigated sizes, but the difference between methanol and water decreases with increasing number of solvent molecules. This indicates that the preference for water will appear for larger clusters.

In summary, our results indicate that although the smallest ion-solvent clusters exhibits a qualitatively opposite behavior form the bulk (where water is a better solvent for ions than methanol), by adding more solvent molecules the bulk order eventually prevails.

List of abbreviations

AAE	Adiabatic association energy
AO	Atomic orbital
aug-cc-pVDZ	Dunning's basis set of Double Zeta quality containing diffuse functions
aug-cc-pVTZ	Dunning's basis set of Triple Zeta quality containing diffuse functions
B3LYP	Becke 3-Parameter (Exchange), Lee, Yang and Parr (correlation; DFT)
BSSE	Basis set superposition error
CID	Collision-induced dissociation
CP	Counterpoise
CBS	Complete basis set limit
cc-pVTZ	Dunning's basis set of Triple Zeta quality
CC	Coupled cluster
CID	Collision-induced dissociation
CCSD(T)	Coupled Cluster theory calculating single and double excitations and taking triple excitations from MP4
DFT	Density functional theoy
EFP	Effective fragment potential
HF	Hartree-Fock Theory
HPMS	High pressure mass spectrometry
m	methanol
MC	Monte Carlo
MD	Molecular dynamics
MO	Molecular orbital
MP2	Møller Plesset perturbation theory
PHPMS	Pulsed ionization beam high pressure mass spectrometry
VAE	Vertical association energy
w	water
ZPVE	Zero-point vibrational energy
ZTRID	Zero-pressure thermal radiation induced dissociation

References

[1] O.M. Cabarcos, C.J. Weinheimer, T.J. Martínez, J.M. Lisy, J. Chem. Phys. 110 (1999) 9516.

[2] K. Hiraoka, S. Mizuse, S. Yamabe, J. Phys. Chem. 92 (1988) 3943.

[3] Gaussian 03, Revision C.02, M. J. Frisch, G. W. Trucks, H. B. Schlegel, G. E. Scuseria, M. A. Robb, J. R. Cheeseman, J. A. Montgomery, Jr., T. Vreven, K. N. Kudin, J. C. Burant, J. M. Millam, S. S. Iyengar, J. Tomasi, V. Barone, B. Mennucci, M. Cossi, G. Scalmani, N. Rega, G. A. Petersson, H. Nakatsuji, M. Hada, M. Ehara, K. Toyota, R. Fukuda, J. Hasegawa, M. Ishida, T. Nakajima, Y. Honda, O. Kitao, H. Nakai, M. Klene, X. Li, J. E. Knox, H. P. Hratchian, J. B. Cross, C. Adamo, J. Jaramillo, R. Gomperts, R. E. Stratmann, O. Yazyev, J. Austin, R. Cammi, C. Pomelli, J. W. Ochterski, P. Y. Ayala, K. Morokuma, G. A. Voth, P. Salvador, J. J. Dannenberg, V. G. Zakrzewski, S. Dapprich, A. D. Daniels, M. C. Strain, O. Farkas, D. K. Malick, A. D. Rabuck, K. Raghavachari, J. B. Foresman, J. V. Ortiz, Q. Cui, A. G. Baboul, S. Clifford, J. Cioslowski, B. B. Stefanov, G. Liu, A. Liashenko, P. Piskorz, Komaromi, R. L. Martin, D. J. Fox, T. Keith, M. A. Al-Laham, Y. Peng, A. Nanayakkara, M. Challacombe, P. M. W. Gill, Johnson, W. Chen, M. W. Wong, C. Gonzalez, and J. A. Pople, Gaussian, Inc., Wallingford CT, 2004.

[4] T. Helgaker, W.Klopper, H. Koch, J. Noga, J.Chem. Phys. 106 (1997) 9639.

[5] H. Koch, B. Fernandez, O. Christiansen, J. Chem. Phys. 108 (1998) 2784.

[6] P. Jurecka, P.Hobza, Chem. Phys. Lett. 365 (2002) 89.

[7] J.H. Choi, K.T. Kuwata, Y.B. Cao, M. Okumura J. Phys. Chem. A 102 (1998) 503.

[8] M. Masamura, J. Chem. Phys. A 106 (2002) 8925.

[9] S.S. Xantheas, J. Phys. Chem. 100 (1996) 9703.

[10] S.S. Xantheas, T.H. Dunning, Jr. J. Phys. Chem. 98 (1994) 13489.

[11] J. Baik, J. Kim, D. Majumdar, K.S. Kim, J. Chem. Phys. 110 (1999) 916.

[12] C.A. Corbett, T.J. Martínez, J.M. Lisy, J. Phys. Chem A 106 (2002) 10015.

[13] C. J. Weinheimer, J.M. Lisy, J. Phys. Chem. 100 (1996) 15305.

[14] O.M. Cabarcos, C.J. Weinheimer, J.M. Lisy, S.S. Xantheas, J. Chem. Phys. 110 (1999) 5.

[15] Džidić, P. Kebarle, J. Phys. Chem. 74 (1970) 1466.

[16] M. Arshadi, R. Yamdagni, P. Kebarle, J. Phys. Chem. 74 (1970) 1475.

[17] B.C. Guo, B. J. Conklin, A.W. Castleman, Jr., J. Am. Chem. Soc. 111 (1989) 6506.

[18] D. H. Evans, R. G. Keesee, A. W. Castleman, Jr. J. Phys. Chem. 95 (1991)3558.

[19] K. Hiraoka, S. Mizuse, S. Yamabe, J. Phys. Chem. 92 (1988) 3943.

[20] S.B. Nielsen, M. Masella, P. Kebarle, J. Phys. Chem. A 103 (1999) 9891.

[21] B.Bogdanov, M. Peschke, D.S. Tonner, J.E. Szulejko, T.B. McMahon, I. J. Mass Spectrom. 185/186/187 (1999) 707.

[22] R.C. Dunbar, T.B. McMahon, D. Thölman, D.S. Tonner, D.R. Salahub, D. Wei, J. Am. Chem Soc. 117 (1995) 12819.

[23] M T. Rodgers, P.B. Armentrout, J. Phys. Chem A 103 (1999) 4955.

[24] P.B. Armentrout, M.T.Rodgers, J. Phys. Chem. A 104 (2000) 2238.

[25] J.C. Amicangelo, P.B. Armentrout, Int. J. Mass Spectrom., 212 (2001) 301.

[26] T.D. Fridgen, T.B. Mc Mahon, P. Maitre, J. Lemaire, Phys. Chem. Chem. Phys. 8 (2006) 2483.

[27] J.E. Combariza, N.R. Kestner J. Phys. Chem. 98 (1994) 3513.

[28] S.S.Xantheas, L.X.Dang, J. Phys. Chem. 100 (1996) 3989.

[29] P. Weis, P.R. Kemper, M.T.Bowers, S.S. Xantheas, J. Am. Chem. Soc. 121 (1999) 35.

[30] R.A. Bryce, M.A. Vincent, N.O.J. Malcolm, I.H. Hiller N.A. Burton, J. Chem. Phys. 109 (1998) 3077.

[31] R.A. Bryce, M.A. Vincent, I.Hillier, J. Phys. Chem. A 103 (1999) 4094.

[32] J.E. Combariza, N.R. Kestner, J. Jortner, Chem. Phys. Let 203 (1993) 423.

[33] J.E. Combariza, N.R. Kestner, J. Jortner, J. Chem. Phys. 100 (1994) 2851.

[34] R.J. Hall, I.H. Hillier, M.A. Vincent, Chem. Phys. Lett. 320 (2000) 139.

[35] T. Asada, K. Nishimoto, K.Kitaura, J. Phys. Chem. 97 (1993) 7724.

[36] D.D. Kemp, M.S. Gordon, J. Phys. Chem. A 109 (2005) 7688.

[37] L. Perera, M.L. Berkowitz, J. Chem. Phys. 100 (1994) 3085.

[38] B. Bogdanov, T.B. McMahon, J. Phys. Chem. A 104 (2000) 7871.

[39] García-Muruais, E.M. Cabaleiro-Lago, J.M. Hermida-Ramón,M.A. Ríos, Chem. Phys. 254 (2000) 109.

[40] C.J. Cramer, Essentials of Computational Chemistry, 2004 Willey & Sons.

[41] J.J. Grabowski, C.H. DePuy, V.M. Bierbaum, J. Am. Chem. Soc. 105 (1983) 2565.

[42] T.H Dunnig, Jr., J. Chem. Phys. 90 (1989) 1007.

[43] J. A. Pople, In Modern Theoretical Chemistry, H.F. Schaefer, III. Ed., Plenum: New York, 1976, Vol. 4.

[44] R. Krishnan, J.S. Binkley, R. Seeger, J.A. Pople, J. Chem. Phys. 72 (1980) 650.

[45] M.J. Freisch, J.A. Pople, J.S. Binkley, J. Chem. Phys. 80 (1984) 3265.

Appendix

Eva Pluhařová and Pavel Jungwirth, “The onset of ion solvation by ab initio calculations: Comparison of water and methanol”, Col. Czechoslovak Chem. Commun., in press (2008)

The onset of ion solvation by ab initio calculations: Comparison of water and methanol

Eva Pluhařová and Pavel Jungwirth*

Institute of Organic Chemistry and Biochemistry, Academy of Sciences of the Czech Republic and Center for Biomolecules and Complex Molecular Systems, Flemingovo nám. 2, 166 10 Prague 6, Czech Republic

*Corresponding author. E-mail: pavel.jungwirth@uochb.cas.cz, FAX: +420-220 410 320

Summary

Optimal structures as well as vertical and adiabatic desolvation energies for sodium cation and fluoride and chloride anions in clusters with one to three water or methanol molecules are determined using converging ab initio methods (MP2/aug-cc-pvtz for geometries and CCSD(T) in the complete basis set limit for energetics). The results, which are in good agreement with previous calculations and experiments (if available), show that in small clusters the interactions of ions with methanol are stronger than those with water. Only upon adding more solvent molecules the situation starts to revert, approaching thus the bulk limit where water is a better solvent for alkali metal cations and halide anions than methanol.

Keywords: clusters, ion solvation, ab initio calculations.

Dedicated to Professor Rudolf Zahradník on the occasion of his 80th birthday.

I. INTRODUCTION

Microsolvation of ions in clusters is often viewed as a tool for approaching the bulk limit[1,2]. Indeed, extrapolation schemes have been applied to elucidate bulk information such as solvation enthalpies and free energies from data obtained for clusters of increasing size[1,2], despite possible pitfalls. These are for example the slow convergence with cluster size to the bulk limit and sizable differences in ion solvation in a liquid at ambient temperature vs. cryogenic clusters. Here, we turn this extrapolation approach upside down asking ourselves how relevant the information about bulk ion solvation is for the situation in small clusters. More precisely, we are posing the following question: If one has two solvents of different dielectric permitivities, such as water with $\varepsilon_r = 80$ and methanol with $\varepsilon_r = 33$, would favorable ion solvation in the bulk medium with a higher dielectric permitivity (i.e., water) translate to stronger interactions in the corresponding small clusters?

Small water clusters with a halide anion or alkali metal cation have been studied extensively in recent decades. A recent density functional theory (DFT) study compares microhydrated structures of these ions in aqueous clusters with up to six water molecules[3]. Alkali metal cations such as sodium or potassium typically exhibit a roughly symmetric water solvent shell[4]. Ab initio calculations of microhydration of halides show a gradual build-up of an asymmetric solvent shell around the anion with the exception of F^- which exhibits a more symmetric mode of solvation[5-14]. Computational studies also exist concerning halide ion solvation in binary clusters with methanol and other short-chain alcohols[15]. Solvation of fluoride and chloride anions in small to medium-size methanol clusters was investigated by a combination of ab initio calculations and vibrational predissociation spectroscopy with the focus on surface vs. interior solvation of the anion[16-17]. Microhydration of alkali metal cations was studied in methanol and other short-chain alcohols and dissociation enthalpies were established[18,19]. In addition, sodium cation - water, sodium cation - methanol, and sodium cation - ethanol dimers were characterized using DFT calculations and IR spectroscopy[20]. Replacement

of water by methanol was found to be exothermic in binary complexes with a sodium cation[21]. Similarly, small clusters of potassium cation with water, methanol, or acetonitrile were characterized[22] and preference of methanol over water as a microsolvent was established[23]. Nevertheless, to the best of our knowledge ion solvation proceses in water and methanol in size selected clusters have not been systematically compared with each other with the aim to answer the question concerning transferability of bulk solvation preferences between the two solvents to small clusters. The goal of the present study is to address this issue by means of accurate ab initio calculations of small ion-water and ion-methanol clusters.

II. SYSTEMS AND COMPUTATIONAL METHODS

Ab initio calculations were performed for small aqueous and methanolic clusters containing a single sodium cation, or fluoride or chloride anion and one to three solvent molecules. Initial structures were chosen using chemical intuition and HF/3-21g pre-optimizations. Optimal structures were then obtained and frequency analysis was performed at the MP2/aug-cc-pVTZ level of theory. For each cluster we additionally evaluated the total electronic energy at MP2/aug-cc-pVTZ and CCSD(T)/aug-cc-pVDZ levels. This allowed for a complete basis set extrapolation (CBS)[24,25] of the form (the numerical constant coming from Ref. 26):

$$E_{\mathrm{MP2/CBS}} = E_{\mathrm{MP2/aug\text{-}cc\text{-}pVDZ}} + (E_{\mathrm{MP2/aug\text{-}cc\text{-}pVTZ}} - E_{\mathrm{MP2/aug\text{-}cc\text{-}pVDZ}})/0.703704 \quad (1)$$

and

$$E_{\mathrm{CCSD(T)/CBS}} = E_{\mathrm{MP2/CBS}} + (E_{\mathrm{CCSD(T)/aug\text{-}cc\text{-}pVDZ}} - E_{\mathrm{MP2/aug\text{-}cc\text{-}pVDZ}}) \; . \quad (2)$$

Using the above extrapolation we evaluated the ion and water or methanol desolvation energies. These were calculated as diferences between the cluster energies with and without the ion or a single solvent molecule, either allowing (adiabatic desolvation energy) or not allowing (vertical

desolvation energy) for cluster relaxation upon removal of ion or solvent molecule. For each system, the adiabatic desolvation energy was corrected for the zero point vibrational energy diference, while the vertical desolvation energy was corrected for the basis set superposition error using the counterpoise scheme[27].

For the smallest clusters containing an ion and a single solvent molecule we verified the employed CBS extrapolation against calculations employing large aug-cc-pVQZ and aug-cc-pV5Z basis sets. Bionding energies obtained this way were within 1 kcal/mol of the values from the original extrapolation. For these systems, we also checked the performance of density functional methods at the BLYP and B3LYP levels of theory, which we found to be almost quantitative. All calculations were performed using the Gaussian 03 program[28].

III. RESULTS AND DISCUSSION

The structures of the optimized ion-water clusters under study are presented in Fig. 1, while those with methanol as a microsolvent are shown in Fig. 2. In both cases we see a similar ion-solvent binding pattern – an anion forms a strong hydrogen bond with each of the solvent molecules, while a cation binds to water oxygens. For methanol clusters, the ion-solvent binding saturates all available OH groups, while in water there remains the possibility of formation of additional solvent-solvent hydrogen bonds. For steric reasons dictated by strong ion-water interactions these additional hydrogen bonds cannot develop for the sodium cation solute. For anions (in particular chloride), water-water hydrogen bonds do exist in the two- and three-water clusters; however, they are strained and, therefore, rather weak.

To further characterize the cluster we evaluated the following energetic properties: the vertical and adiabatic dissociation energies of the solvent molecule and the vertical and adiabatic dissociation energies of the ionic solute. The first two energies are associated with the process

$X(Sol)_n$ —> $X(Sol)_{n-1}$ + Sol, where X is the ion and Sol is the solvent molecule. For evaluation of the vertical dissociation energy the structure of $X(Sol)_{n-1}$ is assumed as unrelaxed after dissociation, while the adiabatic dissociation energy corresponds to a geometrically relaxed fragment $X(Sol)_{n-1}$. Vertical and adiabatic dissociation energies of the ion are associated with the process $X(Sol)_n$ —> $(Sol)_n$ + X. Similarly as in the previous case, for evaluation of the vertical dissociation energy we employ an unrelaxed structure of $(Sol)_n$, while for the adiabatic dissociation energy the geometry of $(Sol)_n$ is optimized after dissociation. For all the systems under study, these dissociation energies are presented in Figs. 3-5. Since our values are obtained at the CCSD(T)/CBS level, they represent a benchmark to previous calculations (discussed in the introduction), with which they are in good agreement whenever available.

Figure 3 summarizes all the investigated dissociation energies for the chloride-containing clusters under study. While the vertical water binding decreases with cluster size (Fig. 3a), the vertical ion binding increases almost linearly, which indicates a close contact of the ion with the first few solvent molecules. The adiabatic curves are less straightforward since the relaxation of the rest of the system after solvent or ion removal comes into play, too.

In the smallest cluster, i.e., the ion-solvent dimer, binding is stronger in methanol than in water. Also for two solvent molecules, binding remains stronger in the methanol case, albeit the difference between the two solvents decreases. The most interesting situation appears in clusters with three solvent molecules where binding of a water molecule (both vertical and adiabatic) becomes stronger than that of a methanol molecule. Nevertheless, ion binding remains stronger for methanol solute; however, the difference from water all but disappears in the adiabatic picture. These results indicate that although the smallest clusters exhibit a qualitatively opposite behavior to that of the bulk (where water is a better solvent for ions than methanol), further

solvent molecules help to restore the bulk order. This is primarily since water unlike methanol can form additional hydrogen bonds in small ion-solvent clusters, which leads to additional stabilization of aqueous clusters with more than a single solute molecule.

The corresponding results for fluoride are depicted in Fig. 4. Although qualitatively the binding pattern is similar to that of chloride, fluoride interacts with solvent molecules more strongly due to its smaller size and, therefore, higher charge density. In addition, the crossover from preference for methanol to water does not occur within the investigated system sizes (except for the vertical solvent binding which becomes practically equal for methanol and water in clusters with three solvent molecules).

Finally, Fig. 5 shows the binding energies for small sodium cation - water and sodium cation - methanol clusters. The strength of binding to sodium cation lies between those to fluoride and chloride, albeit closer to the former. As is the case for the anions, methanol wins as a preferred microsolvent for Na^+ over water. As a matter of fact, there is no reversal of this pattern for the systems under study and larger clusters are needed for flipping the preference to the water side. This is due to the fact that the geometry of water binding to cations does not allow for formation of stabilizing water-water hydrogen bonds in small clusters.

For clarity and easy comparison with previous studies, all the above binding energies are also summarized numerically in Tables 1-3.

IV. CONCLUSIONS

We have presented optimal structures and vertical and adiabatic binding energies of ions and solvent molecules in clusters of sodium cation, fluoride or chloride in clusters with one to three water or methanol molecules. These energies are based on CCSD(T) results at the complete

basis set limit. We show that, contrary to expectations based on extrapolation from the bulk, in the smallest clusters interactions of ions with methanol are stronger than those with water. Only in larger clusters with more solvent molecules the situation is reversed, approaching eventually the bulk situation, where water is a better solvent than methanol for atomic cations and anions.

Acknowledgements

Support from the Czech Science Foundation (grant 203/07/1006) and from the Ministry of Education (grant LC512) is gratefully acknowledged. We thank the *META*Centrum in Brno for generous allocation of computer time.

Supplementary material

All geometric parameters and absolute ab initio energies of the investigated systems are available from the authors on request.

References:

1. Tissandier, M. D., Cowen K. A., Feng W. Y., Gundlach E., Cohen M. H., Earhart A. D., Coe J. V.: *J. Phys. Chem. A* **1998**, *102*, 7787.
2. Meot-Ner M.: *Chem. Rev.* **2005**, *105*, 213.
3. Krekeler C., Hess B., Delle Site L.: *J. Chem. Phys.* **2006**, *125*, 054305.
4. Patwari G. N., Lisy J. M.: *J. Chem. Phys.* **2006**, *118*, 8555.
5. Combariza J. E., Kestner N. R.: *J. Phys. Chem.* **1994**, *98*, 3513.
6. S. S. Xantheas, L. X. Dang: *J. Phys. Chem.* **1996**, *100*, 3989.
7. Bryce R. A., Vincent M. A., Malcom N. O. J., Hiller I. H., Burton N. A.: *J. Chem. Phys.* **1998**, *109*, 1998.
8. Cabarcos O. M., Weinheimer C. J., Lisy J. M., Xantheas S. S.: *J. Chem. Phys.* **1999**, *110*, 5.
9. Baik J., Kim J., Majumdar D., Kim K. S.: *J. Chem. Phys.* **1999**, *110*, 9116.
10. Weis P., Kemper P. R., Bowers M. T., Xantheas S. S.: *J. Am. Chem. Soc.* **1999**, *121*, 3531.
11. Tobias D., Jungwirth P., Parrinello M.: *J. Chem. Phys.* **2001**, *114*, 7036.
12. Masamura M.: *J. Phys. Chem. A* **2002**, *106*, 8925.
13. Zhan C. G., Dixon D. A.: *J. Phys. Chem. A* **2004**, *108*, 2020.
14. Kemp D. D., Gordeon M. S.: *J. Phys. Chem. A* **2005**, *109*, 7688.
15. Bogdanov B., McMahon T. B.: *J. Phys. Chem. A* **2000**, *104*, 7871.
16. Cabarcos O. M., Weinheimer C. J., Martinez T. J., Lisy J. M.: *J. Chem. Phys.* **1999**, *110*, 9516.
17. Corbett C. A., Martinez T. J., Lisy J. M.: *J. Phys. Chem. A* **2002**, *106*, 10015.
18. Rodgers M. T., Armentrout P. B.: *J. Phys. Chem. A* **1999**, *103*, 4955.

19. Garcia-Muruais A., Cabaleiro-Lago E. M., Hermida-Ramon J. M., Rios M. A.: *Chem. Phys.* **2000**, *109*, 254.

20. Fridgen T. D., McMahon T. B., Maitre P., Lemaire J.: *Phys. Chem. Chem. Phys.* **2006**, *8*, 2483.

21. Nielsen S. B., Masella M., Kebarle P.: *J. Phys. Chem. A* **1999**, *103*, 9891.

22. Islam M. S., Pethrick R. A., Pugh D.: *J. Phys. Chem. A* **1998**, *102*, 2201.

23. Evans D. H., Keesee R. G., Castelman A. W. Jr.: *J. Phys. Chem.* **1991**, *95*, 3558.

24. Feller D.: *J. Chem. Phys.* **1992**, *96*, 6104.

25. Feyereisen M. M., Feller D., Dixon D. A.: *J. Phys. Chem.* **1996**, *100*, 2993.

26. Helgaker T., Klopper W., Koch H., Noga J.: *J. Chem. Phys.* **1997**, *106*, 9639.

27. Boys S. F., Bernardi F.: *Mol. Phys.* **1970**, *19*, 558.

28. Gaussian 03, Revision C.02, Frisch M. J., Trucks G. W., Schlegel H. B., Scuseria G. E., Robb M. A., Cheeseman J. R., Montgomery Jr. J. A., Vreven T., Kudin K. N., Burant J. C., Millam J. M., Iyengar S. S., Tomasi J., Barone V., Mennucci B., Cossi M., Scalmani G., Rega N., Petersson G. A., Nakatsuji H., Hada M., Ehara M., Toyota K., Fukuda R., Hasegawa J., Ishida M., Nakajima T., Honda Y., Kitao O., Nakai H., Klene M., Li X., Knox J. E., Hratchian H. P., Cross J. B., Bakken V., Adamo C., Jaramillo J., Gomperts R., Stratmann R. E., Yazyev O., Austin A. J., Cammi R., Pomelli C., Ochterski J. W., Ayala P. Y., Morokuma K., Voth G. A., Salvador P., Dannenberg J. J., Zakrzewski V. G., Dapprich S., Daniels A. D., Strain M. C., Farkas O., Malick D. K., Rabuck A. D., Raghavachari K., Foresman J. B., Ortiz J. V., Cui Q., Baboul A. G., Clifford S., Cioslowski J., Stefanov B. B., Liu G., Liashenko A., Piskorz P., Komaromi I., Martin R. L., Fox D. J., Keith T., Al-Laham

M. A., Peng, C. Y., Nanayakkara, A., Challacombe M., Gill P. M. W., Johnson B., Chen W., Wong M. W., Gonzalez, C., Pople J. A.: Gaussian, Inc., Wallingford CT, 2004.

Tables

Table 1a Vertical and adiabatic CCSD(T)/CBS binding energies of a solvent molecule in water (w) or methanol (m) clusters with chloride and one to three solvent molecules.

	E (kcal/mol)			
n	vertical w	adiabatic w	vertical m	adiabatic m
1	-15.53	-14.10	-17.24	-16.58
2	-15.53	-13.28	-15.65	-15.16
3	-16.94	-13.61	-14.04	-12.62

Table 1b Vertical and adiabatic CCSD(T)/CBS binding energies of chloride in water (w) or methanol (m) clusters with one to three solvent molecules.

	E (kcal/mol)			
n	vertical w	adiabatic w	vertical m	adiabatic m
1	-15.53	-14.10	-17.24	-16.58
2	-28.99	-24.72	-31.48	-27.01
3	-40.66	-28.39	-44.24	-29.54

Table 2a Vertical and adiabatic CCSD(T)/CBS binding energies of a solvent molecule in water (w) or methanol (m) clusters with fluoride and one to three solvent molecules.

	E (kcal/mol)			
n	vertical w	adiabatic w	vertical m	adiabatic m
1	-32.67	-27.27	-36.42	-31.31
2	-23.29	-18.59	-24.68	-20.96
3	-20.10	-16.13	-19.55	-16.33

Table 2b Vertical and adiabatic CCSD(T)/CBS binding energies of fluoride in water (w) or methanol (m) clusters with one to three solvent molecules.

	E (kcal/mol)			
n	vertical w	adiabatic w	vertical m	adiabatic m
1	-32.67	-27.27	-36.42	-31.31
2	-52.04	-43.16	-55.32	-47.47
3	-67.75	-51.55	-72.15	-53.70

Table 3a Vertical and adiabatic CCSD(T)/CBS binding energies of a solvent molecule in water (w) or methanol (m) clusters with sodium and one to three solvent molecules.

	E (kcal/mol)			
n	vertical w	adiabatic w	vertical m	adiabatic m
1	-22.36	-20.92	-24.46	-23.22
2	-19.87	-18.59	-21.35	-20.40
3	-17.06	-15.29	-18.04	-16.38

Table 3b Vertical and adiabatic CCSD(T)/CBS binding energies of sodium in water (w) or methanol (m) clusters with one to three solvent molecules.

	E (kcal/mol)			
n	vertical w	adiabatic w	vertical m	adiabatic m
1	-22.36	-20.92	-24.46	-23.22
2	-42.76	-36.44	-46.29	-38.62
3	-61.17	-44.00	-65.17	-44.91

Figure Captions

Figure 1: Structures of ion-water clusters for chloride, fluoride, and sodium with one to three water molecules.

Figure 2: Structures of ion-methanol clusters for chloride, fluoride, and sodium with one to three water molecules.

Figure 3: Vertical and adiabatic CCSD(T)/CBS binding energies of a) solvent and b) chloride in water (w) or methanol (m) clusters with one to three solvent molecules.

Figure 4: Vertical and adiabatic CCSD(T)/CBS binding energies of a) solvent and b) fluoride in water (w) or methanol (m) clusters with one to three solvent molecules.

Figure 5: Vertical and adiabatic CCSD(T)/CBS binding energies of a) solvent and b) sodium in water (w) or methanol (m) clusters with one to three solvent molecules.

Figure 1

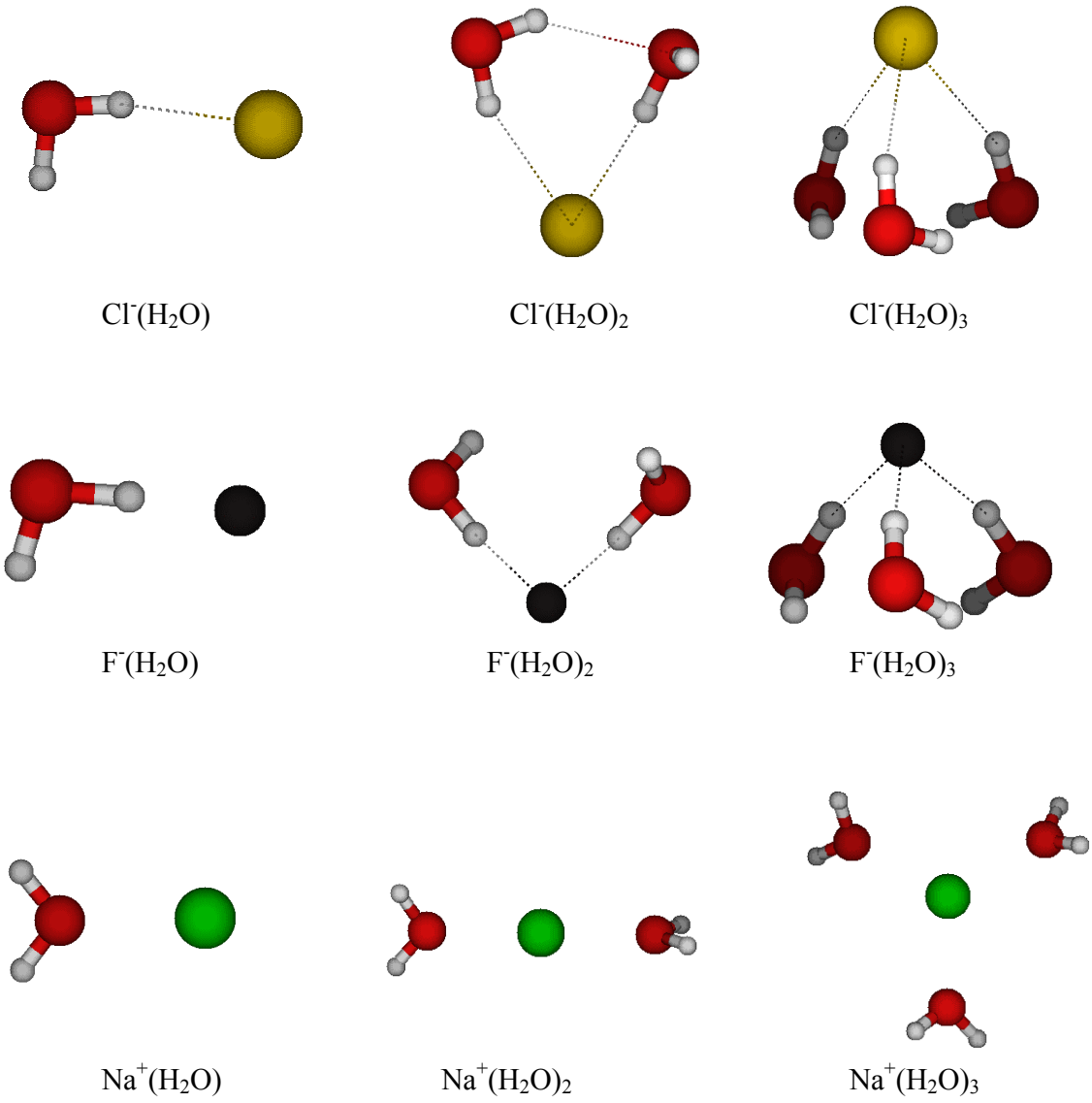

Figure 2

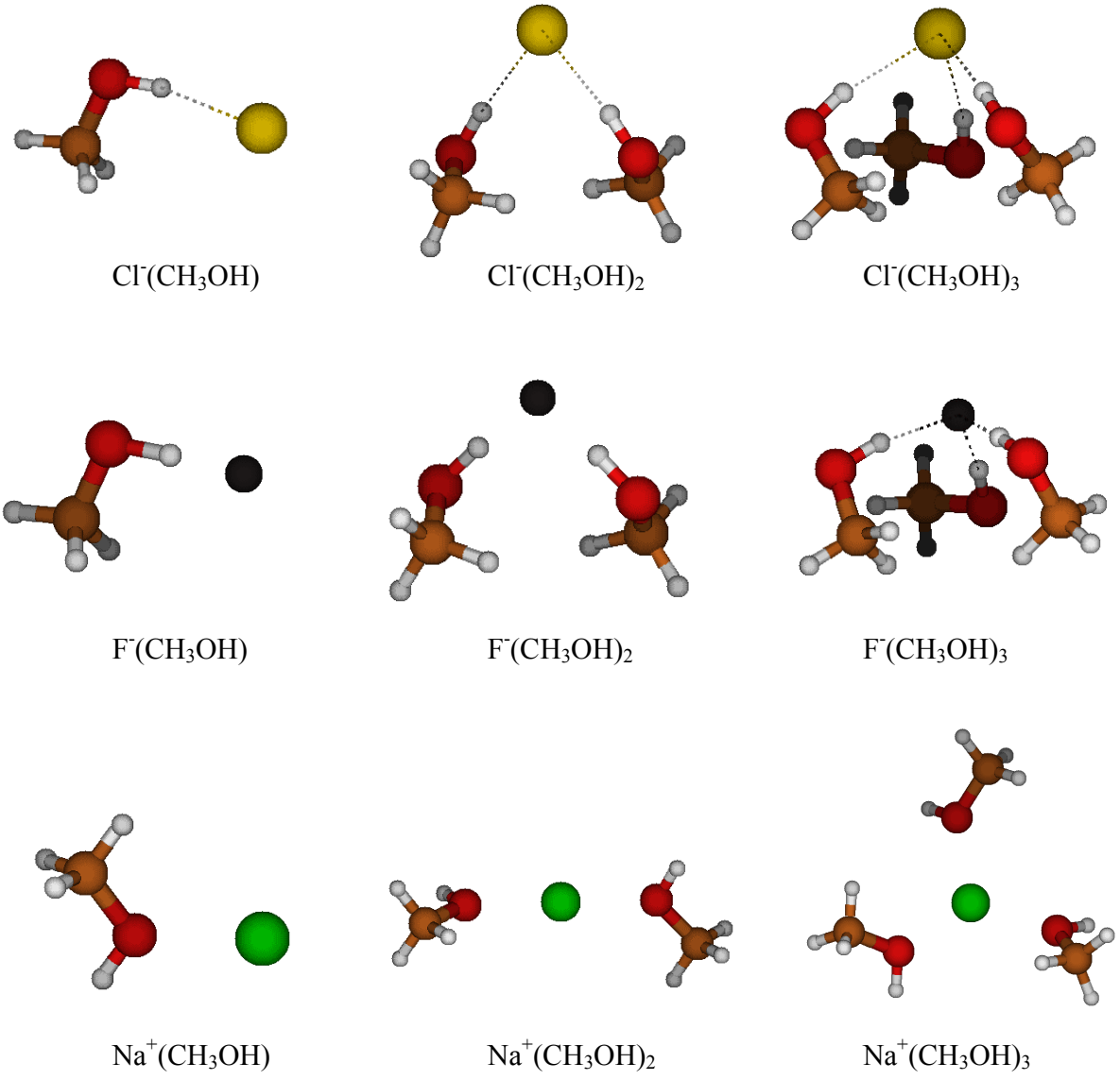
$Cl^-(CH_3OH)$
$Cl^-(CH_3OH)_2$
$Cl^-(CH_3OH)_3$
$F^-(CH_3OH)$
$F^-(CH_3OH)_2$
$F^-(CH_3OH)_3$
$Na^+(CH_3OH)$
$Na^+(CH_3OH)_2$
$Na^+(CH_3OH)_3$

Figure 3a:

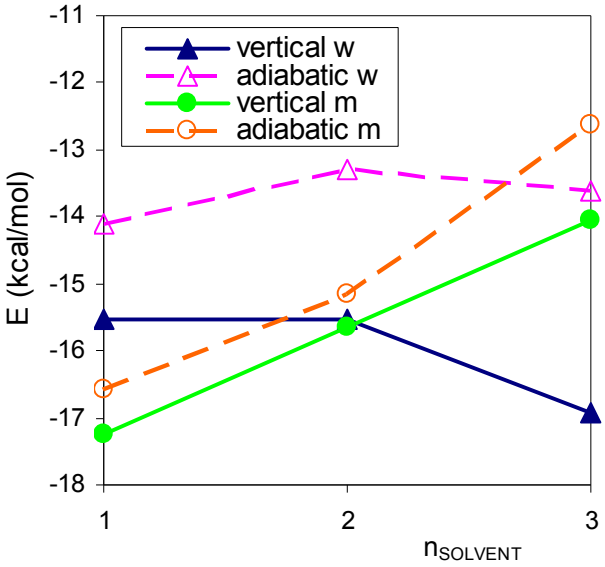

Figure 3b:

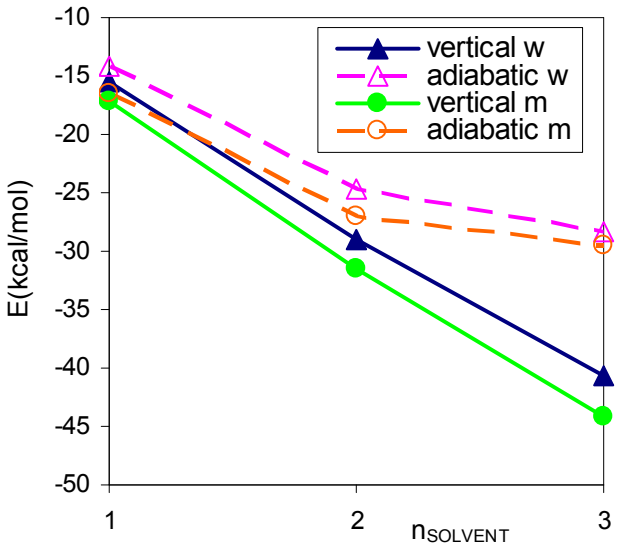

Figure 4a:

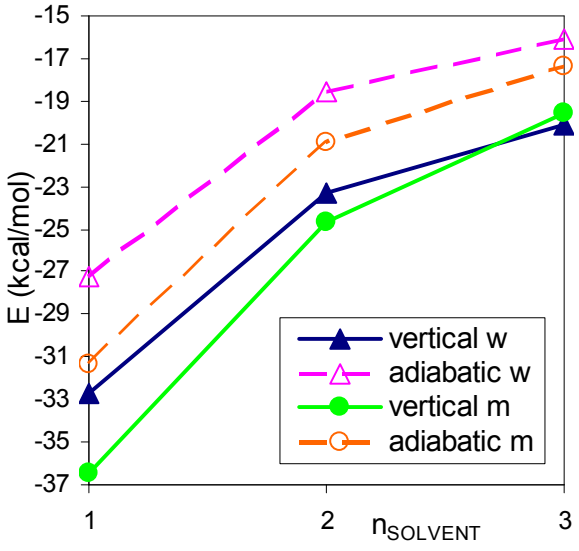

Figure 4b:

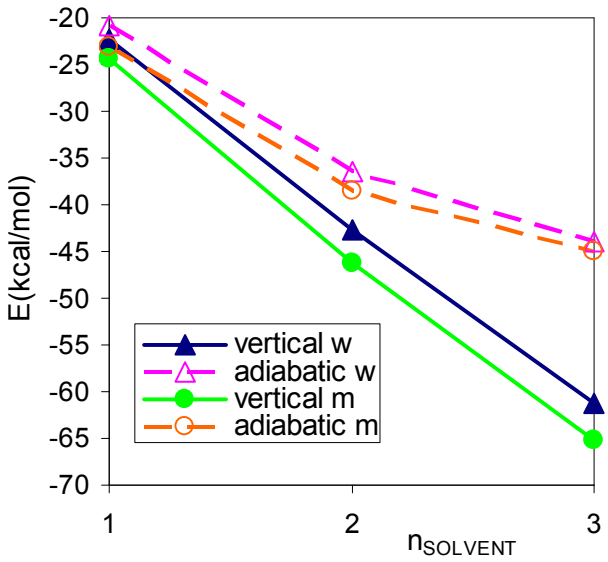

Figure 5a:

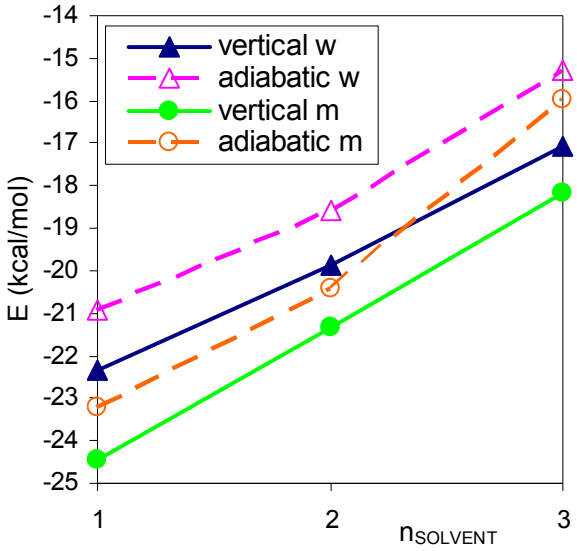

Figure 5b

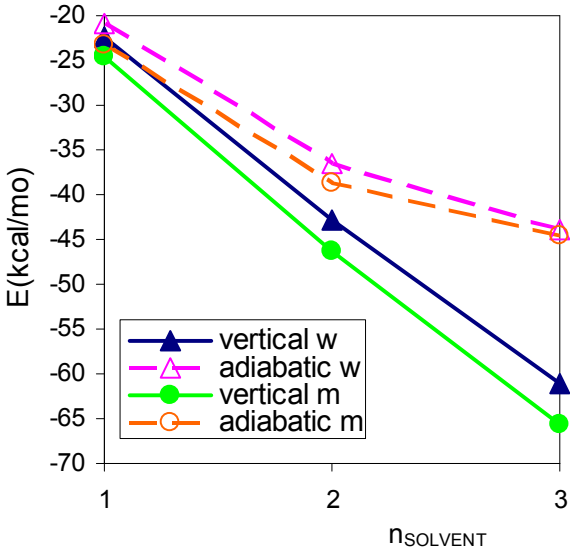

: